University of Alberta

Impact of Solvents Treatment on the Wettability of Froth Solids

by

Fan Yang

A thesis submitted to the Faculty of Graduate Studies and Research
in partial fulfillment of the requirements for the degree of

Master of Science

in

Materials Engineering

Chemical and Materials Engineering Department

Examining Committee

Zhenghe Xu, Chemical and Materials Engineering

Jacob Masliyah, Chemical and Materials Engineering

Lingyun Chen, Agricultural, Food and Nutritional Science

Abstract

The purpose of this study is to investigate the impact of solvent addition to bitumen froth on the wettability of froth solids. The wettability of solids determines the transportation/partitioning of the solids between phases, which in turn affects the solids and water rejection in a Clark hot water extraction process (CHWE).

The impact of solvents treatment on the wettability of froth solids was studied using both a model system and a real bitumen froth system. The vulnerabilities of four kinds of model minerals to hydrocarbon contamination/wettability alteration in different solvents were compared and discussed by considering solvent composition and mineral types.

The wettability of solids extracted from the industrial froth using different solvents was also compared. The XRD analysis on these solids confirmed the partitioning behavior of solids observed in model solids system.

The results from this study indicate that the composition of paraffinic/aromatic solvent in an industrial froth treatment process could be tailor-optimized to achieve a better solids/water rejection.

Acknowledgements

I would like to take this opportunity to thank Professors Zhenghe Xu and Jacob Masliyah for their support and guidance throughout the development of this project. Their instructions are instrumental in my desire and ability in thinking as an engineer.

I also owe much gratitude to Dr. Kevin Moran. During the course of the project, he was always involved, informative and ready to help, his timely guidance and help were critical in keeping me on track in my graduate education. I am lucky to have Mr. Allan Yeung as my lab supervisor, I appreciate for all the assistance he gave me and the rich experience he shared with me.

My sincere appreciation also goes to Dr. Xianhua Feng and Ms.Shiau-Yin Wu. You both are fantastic colleagues, and I am amazed by your hardwork and the will to help people around.

I would like to dedicate this thesis to my parents Jian Yang and Zhijun Huang, and my girlfriend Xiujun Li.

TABLE OF CONTENTS

LIST OF TABLES

LIST OF FIGURES

LIST OF NOMENCLATURE/ABBREVIATION

Anhy	Anhydrite
Cal	Calcite
CEC	Cation Exchange Capacity
Chl	Chlorite
CHWE	Clark Hot Water Extraction
CSS	Combined Solid Samples
Dol	Dolomite
Hep-Dil-Bit	Heptane Diluted Bitumen
Ill	Illite
Kaol	Kaolinite
K-feld	Potassium Feldspar
ML	Mixed-layer clays
OWS	Oil Wettable Solids
Plag	Plagioclase
PSS	Partitioned Solid Samples
PSV	Primary Separation Vessel
Pyr	Pyrite
Qtz	Quartz
Sider	Siderite
Smec	Smectite
Tol-Dil-Bit	Toluene Diluted Bitumen
WWS	Water Wettable Solids
XRD	X-Ray Diffraction

CHAPTER 1 GENERAL INTRODUCTION

The minable oil sands in Alberta contain about 7~14% bitumen, 85% mineral solids and 5% water by weight.[1] Bitumen is high molar mass viscous petroleum, which, after being extracted from the oil sands, can be upgraded into synthetic crude oil, SCO, having an API gravity of about 31 and further fractionated to gasoline, heating oil and diesel fuel in bitumen refining processes.

The oil sands deposit in Alberta, Canada, is the largest bitumen deposit so far discovered in the world. At present, the Alberta oil sands industry covers leases of over 141,000 square kilometres of oil sands, which are mainly within Athabasca, Cold Lake, and Peace River areas. The recovery of bitumen from oil sands is achieved commercially either by surface mining, which mines out oil sands ore located within a depth less than about 50 meters from the ground surface, followed by bitumen extraction or by in-situ extraction of bitumen from oil sands ore buried under typically more than 200 meters from the ground surface.

The Athabasca area was found to hold more than 60% of the oil resources in Province of Alberta. The total volume of remaining reserve for crude bitumen is estimated to be about 27 billion cubic meters or 170.4 billion barrels. Current annual output is 477 million barrels. Based on this exploration rate, the oil resources are able to meet Canada's crude oil needs for the next several centuries.[2]

The extraction of bitumen from oil sands has been extensively studied. In 1920s, Karl Clark invented an extraction method based on the use of hot water, which is the well known 'Clark Hot Water Extraction process' (CHWE).[1] A variation of this process has been widely used in the oil sands industry from its invention to present. Figure 1-1 shows a schematic flow process of bitumen extraction from oil sands.
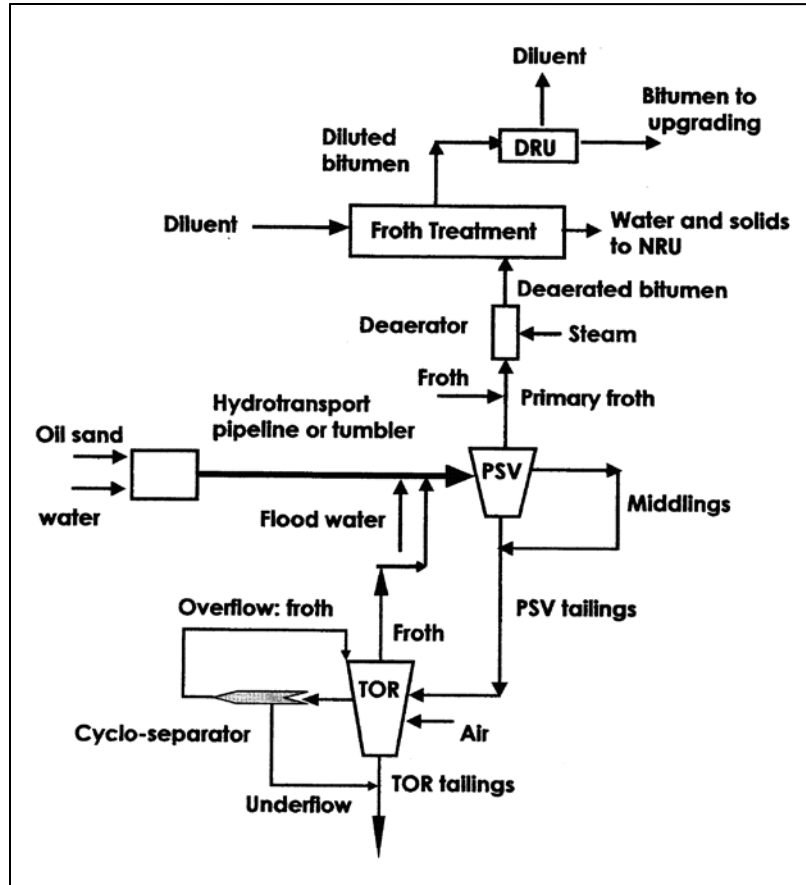
Figure 1-1. Schematic flow sheet of a bitumen extraction process.[3]

In the bitumen extraction process, after oil sands are mined and the oil sand lumps are crushed, they are mixed with hot water under alkaline condition which is achieved by addition of sodium hydroxide.[4] The slurry generated as such is sent to a large primary separation vessel (PSV) through hydro-transport pipelines where bitumen is liberated from the sand grains. In the PSV, aerated bitumen floats to the top of the vessel, whereas most of the solids settle to the bottom of the PSV forming tailings, and most water remains in the middle forming middlings, which contains small amount of bitumen and solids. The liberated floated bitumen has fine solids and water, forming so-called bitumen froth. The bitumen froth is then collected and sent to the froth treatment unit, together with the froth recovered from the middlings stream which was processed in secondary flotation cells. After de-aeration, bitumen froth usually contains 60% bitumen, 30% water and

10% solids by weight. To facilitate removal of the solids and water from the bitumen froth, solvents are usually used to decrease the bitumen froth viscosity and increase the density difference between hydrocarbons and water and solids. In commercial operations, two types of solvents have been used, that is, naphtha and short chain alkanes. The froth treatment technique using naphtha as a diluent is called naphtha froth treatment and the technique using short chain alkanes as a diluent is called paraffinic froth treatment. By using centrifuge and/or inclined plate settlers, the naphtha froth treatment generates a diluted bitumen product with 2─3% water and about 1% of solids. The paraffinic froth treatment, on the other hand, gives a diluted bitumen product with only about 100 ppm of water and almost no solids by gravity settling.[1] After removal of solvents from the diluted bitumen in a diluent recovery unit (DRU), the final clean bitumen is sent to the upgraders to produce synthetic crude oil.

CHAPTER 2 LITERATURE REVIEW

2.1 Introduction to bitumen froth treatment

The bitumen froth treatment process is essentially a cleaning process in which a solvent is used to dilute the bitumen froth to decrease the viscosity and density of the hydrocarbon phase. By using physical separation techniques, most of the solids and water present in the froth would be removed before bitumen is sent to the upgraders.

As stated in Chapter I, two kinds of froth treatment methods are being used in the oil sands industry. Currently, the naphtha-based froth-treatment is used by Syncrude, Suncor and CNRL and the paraffinic froth treatment is used by Shell Albian Sands.[5] In the paraffinic froth treatment, a high solvent to bitumen ratio is employed to trigger the precipitation of asphaltenes from the bitumen. Since asphaltenes precipitate together with solids and water droplets, acting as a flocculent, this method can achieve a nearly clean bitumen product with very small amount of solids and water.[6]

In a typical naphtha-based froth treatment process, the bitumen froth collected from the PSV is fed to the froth treatment plant after bitumen froth-deaeration. In the naphtha-based froth treatment plant, the bitumen froth is first diluted with naphtha to decrease its viscosity and then centrifuged in a scroll type centrifuge at 1100 g to remove the coarse solids and free water.[1] The preliminarily cleaned diluted froth is then sent to disc-nozzel type centrifuges (Alpha-Laval) operating at up to 5500 g to be further cleaned.[1] After the treatment, the final diluted bitumen product has roughly 2% water and 1% solids.[1] The water present in the bitumen product is considerably hard to remove as it is in the form of emulsified water droplets in bitumen of several microns in size.

Figure 2-1 shows micrographs of the naphtha-diluted froth and heptane-diluted froth. In naphtha-diluted froth, many small water droplets are found dispersed in it, whereas in heptane-diluted froth water droplets become larger and form large aggregates with precipitated asphaltenes and solids.
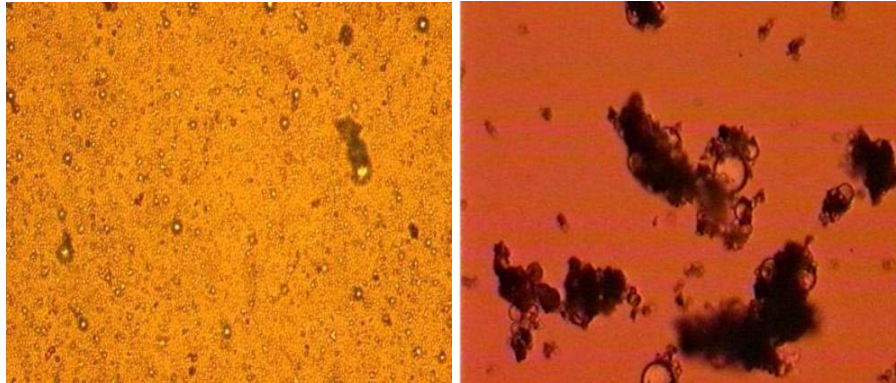
(a) Naphtha diluted froth   (b) Heptane diluted froth
Figure 2-1 Microscopic images of diluted froth. [6]

Both methods have advantages and drawbacks. The high bitumen quality achieved by the paraffinic method is at the cost of a higher usage of a more expensive diluent, which brings important economic and environmental issues. The naphtha-based froth treatment, on the other hand, does not trigger asphaltenes precipitation but suffers from the presence of residual water and fine solids in the product which would lower bitumen quality and limit downstream processing options.

2.2 The nature of froth

The PSV bitumen froth is a mixture of bitumen, water, solids and air. Under a microscope, the morphology of froth contains generally two phases:

1.   An aqueous phase with bitumen droplets dispersed in it and
2.   An aerated hydrocarbon phase with dispersed emulsified water droplets.

A cleaning process is always needed to remove most of the solids and water in the froth before it can be used as a raw material to produce synthetic crude oil. Thus, research is necessary to maximize the recovery of bitumen from the froth while maintaining the best product quality, that is, low water and solids content in the final de-aerated bitumen product.

2.3 Impact of froth solids on bitumen froth treatment

The froth solids have been found to be associated with many issues in froth treatment, such as water-in-oil emulsion break-up, solids rejection and oil droplets coalescence. Thus, a fundamental understanding of the solids type and their behavior in the froth treatment process is crucial to improve the performance of froth treatment in the industrial operation.

2.3.1 Solids type in oil sands

From the very beginning of oil sands extraction research, researchers have been trying to identify the solids type in the oil sands ores and process streams from a mineralogical perspective.

It is now accepted that the mineralogy of solids presented in the oil sands varies across the Athabasca oil sands deposit. Bayliss and Levinson et al.[7] published a review article in 1976 in which they reported the mineralogy of oil sands clays from 247 ore-samples. Their major finding is that kaolinite and illite are the dominant clay type in oil sands, while traces of chlorite and montmorillonite also exist in some of the samples. A number of mineralogical analyses were done on fine solids from the production tailings as well[8,9,10,11] as the mineralogy was believed to be very important in the colloidal interaction in the waste tailings treatment. Kaminsky used X-ray diffraction to characterize mineral distribution in different streams from a batch extraction unit. [12] She observed a depleted amount of illite-smectite clays and an enrichment of kaolinite and iron oxide in the froth as compared to the tailings. This is a very interesting finding since it

suggests that the affinity of clay minerals in oil sands to the water continuous tailings and hydrocarbon continuous froth streams are associated with their mineralogy.

Kaminsky has summarized this research on the clay mineralogy in the oil sands. The summary table is shown in Appendix I.[12]

2.3.2 Implication of solids wettability on solids intractability

The naphtha-based froth treatment process involves dilution of froth by naphtha followed by multi-step centrifugation to remove the water and solids. Typically, after the froth treatment, the final diluted bitumen product contains 2-3% water and 1% solids. The residual water and solids in the bitumen would cause fouling of reactors and poisoning of catalysts in the downstream upgrader.

The paraffinic froth treatment method initially designed by Syncrude researchers is found to be able to achieve a bitumen product that is almost free of solids.[13] However, the high product quality is achieved at a higher cost for bitumen production.

By using toluene dilution and high-speed centrifugation, Kotlyar et al. successfully isolated the fine solids associated with bitumen product.[14] The characterization of these solids revealed that most of them are ultrafine clays with asphaltene-like surface properties. These solids are majorly alumino-silicate in nature with some of them bearing heavy metals.
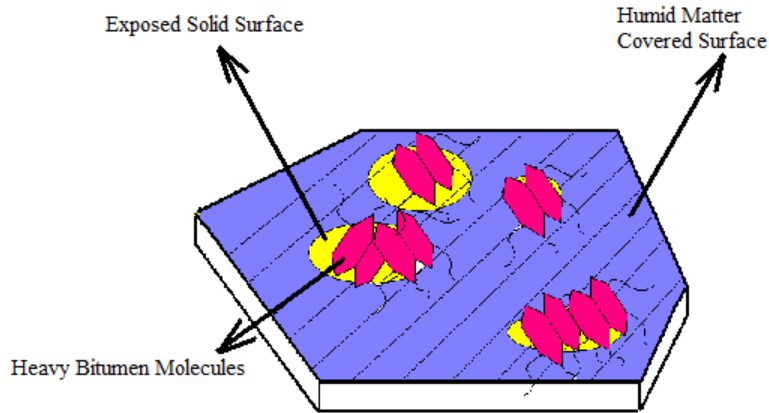
Figure 2-2. A schematic view of clay surface covered by hydrocarbons.

Bensabba et al.[15] proposed that the hydrocarbons interacting with a host solid surface become insoluble in solvents such as toluene. The coverage of the toluene insoluble materials (TIOM) on the surface is in a patchy manner, thus making the solid surface asphaltene-like in nature and suggesting that they could stabilize the emulsified water droplets because they are bi-wettable.

The surface properties of these organic associated solids were studied by Darcovich et al.[16] They used an adhesion method to measure the wettability of those solids and found that the degree of hydrophobicity was directly related to the carbon content on the solid surface.

2.3.3 Implication of solids wettability on oil coalescence

Two phases are generally observed in de-aerated bitumen froth. One phase is the hydrocarbon continuous phase with water droplets dispersed in it and the other phase is the water continuous phase with bitumen droplets dispersed in it. The latter is formed due to the entrainment of bulk water phase into the froth with unliberated bitumen. The bitumen droplets dispersed in water have a higher density because they are attached to bi-wettable solids. Because of the slim coating on surface, these bitumen droplets are hard to be captured by air bubbles. Moreover, these oil droplets entrained in the water phase have less chance to

access solvent in the froth treatment process. As a result, they become the major contributor to the bitumen loss in the tailing streams.

By using kaolinite particles with asphaltene adsorbed at different extent, Yan et al.[17] found that the solids-stabilized oil in water emulsion would have higher average droplets size when the hydrophobicity of the particles was increased. They suggested adding fresh oil droplets to promote the coalescence of the already present oil droplets.
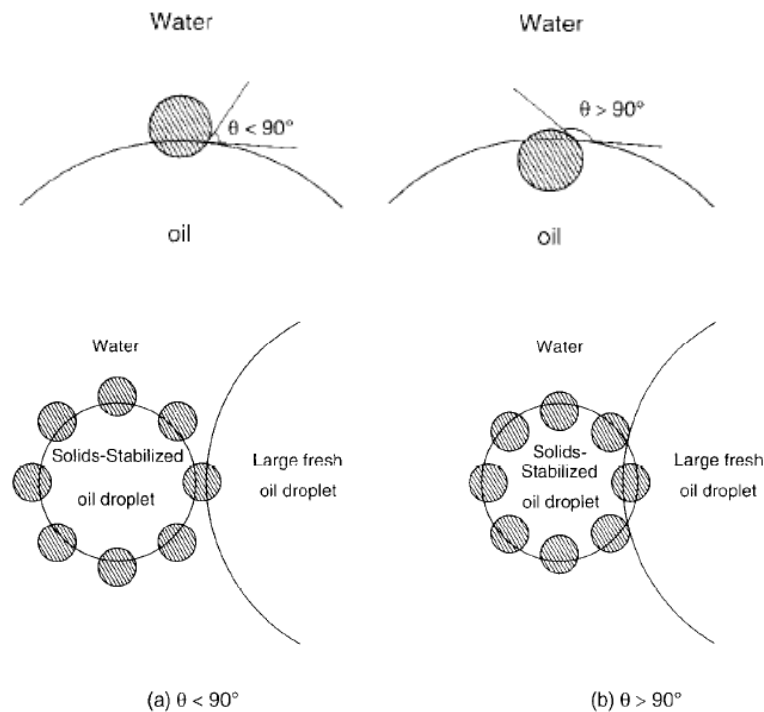
Figure 2-3. Position of solids at the oil/water interface for: (a) hydrophilic solids and (b) hydrophobic solids. [17]

They discussed the mechanism of fresh oil activation based on the hydrophobicity of the solids and their resulting equilibrium position at the oil/water interface. As shown in figure 2-3, for more hydrophilic solids, the equilibrium could be reached before the oil droplets' surfaces meet each other as only a small fraction of the solids volume is needed to be engulfed by the oil droplets to reach equilibrium.

For a more hydrophobic solids however, a large volume of solid particle needs to be engulfed and would finally result in oil coalescence.

2.3.4 Implication of solids wettability on water emulsion stability

2.3.4.1 Intractable water
The dryness of the bitumen product is determined by the stability of the W/O emulsions formed. In a typical naphtha-based froth treatment process, with all the separation techniques, around 2-3% by weight of the water would still remain as emulsified water in the final bitumen product. This part of water, though in a small amount, would be detrimental to the further process as the dissolved salts in it would bring corrosive problems to the downstream upgrading facilities. Many endeavors have been made to understand the stability mechanisms of W/O emulsions and find how to break these emulsions.[18,19,20]

2.3.4.2 Property of the W/O interface
It is widely reported that the stability of W/O emulsions in bitumen froth treatment arises from the steric interfacial film between oil/water interfaces that prevents the water droplets from coalescence.[21] Yeung et al. first introduced the unique micropipette technique to reveal this rigid interfacial film that was responsible for the stability.[22]
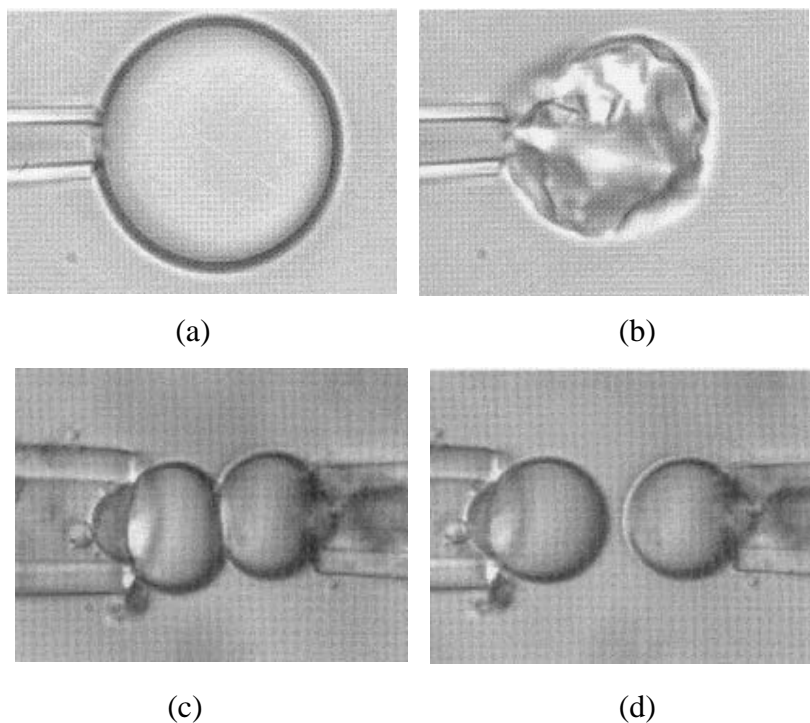
Figure 2-4. Steric nature of the oil/water interface (a) expelled water droplet (b) crumple interface when withdrawing (c) head on head coalescence (d) non-sticky when separate.[22]

By immersing a water filled micropipette into the bitumen in heptol (heptane/ toluene=1/1 by volume) solution, a water droplet was expelled at the tip of the pipette. It was observed that below a bitumen concentration of 1%, the withdrawal of the water droplet would result in a crumpled interface, like a deflated balloon. This would indicate that the oil/water interface has adsorbed material on it. By bringing two droplets together, the film was found to provide a steric effect that prevents the coalescence of these two droplets. For then, upon separation, it was found that they did not "stick" to each other.

While the composition of the interfacial film is still unknown, several agents were proposed as being responsible for the emulsion stability, including asphaltenes,[23] solids,[24] wax and resins.[25]

2.3.4.3 Solids contribution to the Interface stability

Asphaltenes are the most widely reported materials for the interfacial film due to their bi-wettable nature. Thus, in many studies on model-emulsion behaviour, asphaltenes are commonly used as the stabilizing agent.[26,27,28]

The Langmuir-trough studies were carried out to study asphaltene films formed at an oil/water interface.[3] In the tests, asphaltenes were dissolved in toluene and the solution was placed on the top of water surface. After toluene evaporation, a monolayer of asphaltene film was formed on the water surface. It was found that the addition of fresh toluene could not dissolve the asphaltene film, even though asphaltenes are considered soluble in toluene. Surface pressure tests confirmed that the asphaltene film is rigid.

Similar to asphaltene molecules, much of solids in the oilfield are also found bi-wettable due to their natural properties or hydrocarbons contamination.[29] Examples include clays, quartz, calcite, pyrite, etc. These solids would act together with asphaltenes and contribute to the stability of emulsions found in the industry.[30]

By using model water in oil emulsion, Saukowski and Yarranton found that asphaltenes and solids could both adsorb onto the oil/water interface.[30] Their SEM images revealed that the major types of solids adsorbed at the interface are pallet-like clays. By increasing the solids concentration in the system, the fractional surface area covered by solids would increase, and the maximum coverage would reach 50% when the solids concentration in asphaltene solution reached 2.8kg per 1.9kg/m^3 asphaltenes.

A similar observation was found by Yan et al.[24] They studied different bitumen components including asphaltenes, de-asphalted bitumen and fine solids on the stability of water in oil emulsions and found that asphaltenes and solids are the main stabilizer. Their settling tests revealed that the emulsion was more stable when the

two stabilizers were both present rather than a single one of them. Their SEM analysis also indicated that the stabilizing solids are pallet-like clays.
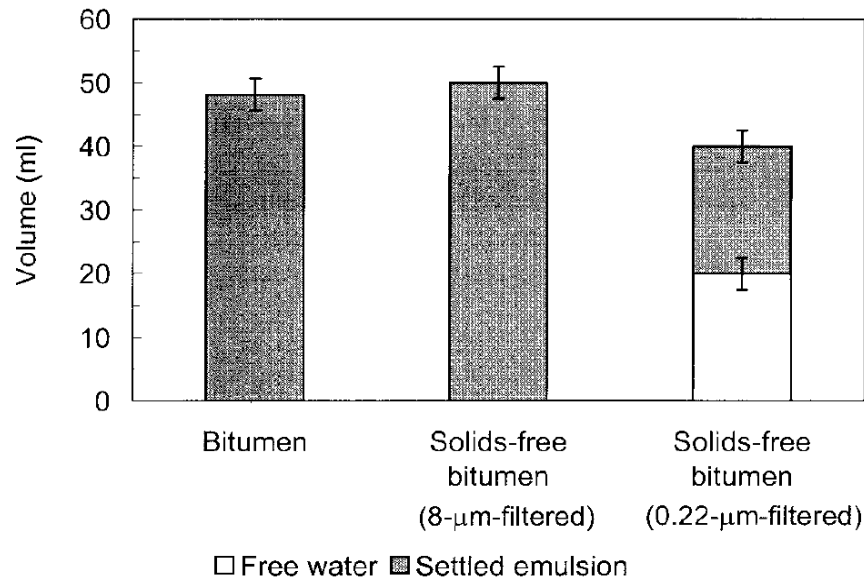
Figure 2-5 Particle size's impact on emulsion stability.[24]

Yan and Elliot's work also suggested that the size of the particles has influence on emulsion stability. Using a filter paper to exact smaller size particles from the bitumen, the emulsion became less stable and free water separated out after 24 hours setting.

The work of Saukowski was later expanded to explore the dependence of emulsion stability on the solids size and coverage ratio of the surface.[31] It was found that the most stable emulsion was only achieved when asphaltenes and solids worked together such that the asphaltenes would immobilize the solids on the surface while the surface solids would make the asphaltenes film rigid. The authors found that the most stable interface was formed when the fractional area coverage ratio of asphaltenes to solids was 2:1.

Poindexter et al.[32] carried experiments to probe the vulnerability of different crude oil emulsion's stability to demulsifiers by changing factors such as asphaltenes, resins, naphthenic acids, solids, aromaticity, metal content, viscosity, and API gravity etc. in the system.
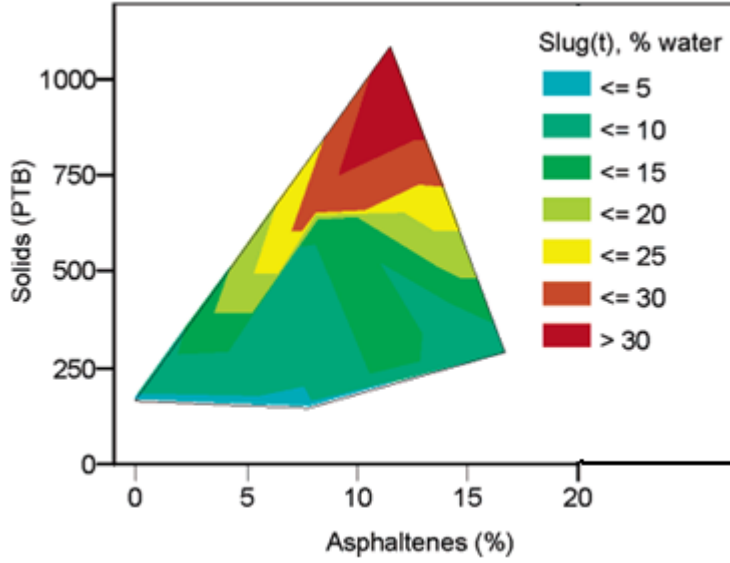
Figure 2-6. The emulsion stability was more influenced by solids than asphaltenes.[32]

They surprisingly found that the solids content had a dominate effect on the emulsion stability over all the other factors including asphaltenes content.

Wu successfully isolated the interfacial organics and mineral solids accumulated at the oil/water interface using a novel technique called selective creaming.[33] The method is shown schematically in figure 2-7.
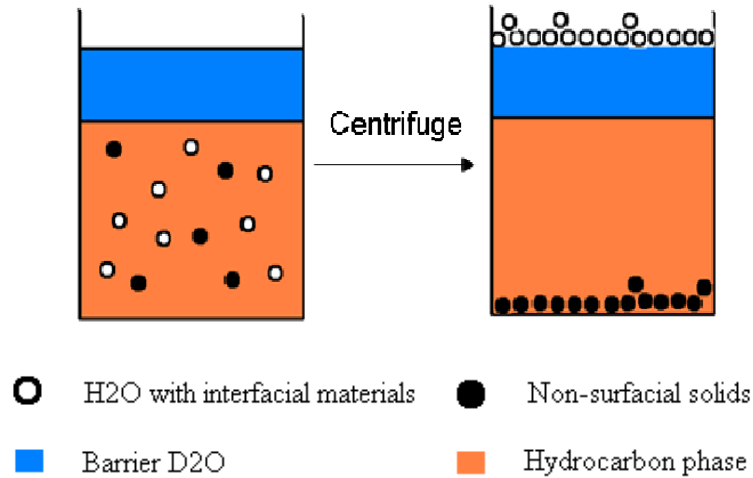
Figure 2-7. Selective creaming method.[33]

This technique used D_2O as a barrier agent and modified the density of the emulsion so that it would be heavier than D_2O. After centrifugation, the water droplets with interfacial materials were collected as the top phase. Characterization of the interfacial materials revealed the composition of the interface contains 32 % of asphaltene and 20.9 % by weight of clay pellets with sizes within 1-3 µm.

2.3.4.4 Implication of solid wettability on emulsion stability

The stability of emulsions by solid particles is largely determined by the ability of solids to move onto the oil/water interface and stay there in an equilibrium state. Thus, an understanding of the wettability of solids in the system is required to better address the issues of emulsions.
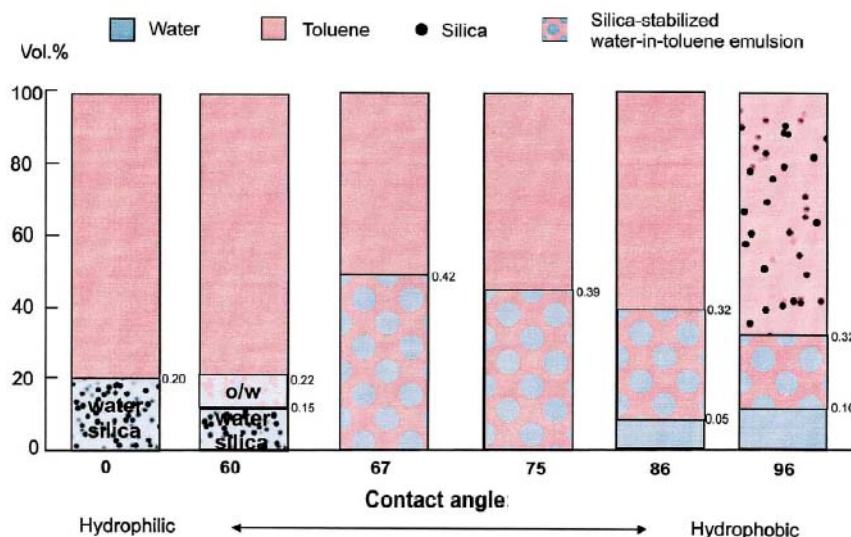
Figure 2-8. Emulsion formation by solids with different wettabilities. [41]

By silanization, fumed silica spheres were rendered to different hydrophobicity and used in Yan et al.'s emulsion stability tests.[41] In their study, water droplets were added in Bayol 35 and an ultrasonic bath was used to produce emulsions. It was found that the formation of emulsion is strongly dependent on the hydrophobicity of the silica spheres. With untreated hydrophilic silica spheres used, no emulsion was formed after sonication and all silica spheres were washed off into the water phase. The largest volume of emulsion was formed when silica spheres with contact angle of 67° were used as the stabilizing solids. Silica spheres with high hydrophobicity (contact angle of 97°) would result in less emulsion volume and solids suspension in the oil phase.

16

2.4 Solids wettability measurement methods

Though the importance of solids' wettability in oil sands extraction is clear, there is little literature to be found on characterizing the wettability of bitumen froth solids. This is probably due to the difficulties in determining the wettability of solids and the sensitivity of the current wettability evaluation methods. Generally, the wettability measurements of solids could fall into two categories, either as a qualitative measurement such as the phase partitioning tests, or a quantitative measurement such as contact angle measurement (CA) or Water Drop Penetration Time tests (WDPT). Several wettability evaluation tests are discussed in this section and the advantage of each of them is evaluated.

2.4.1 Partitioning tests

Partitioning test is the mostly used method for a quick evaluation of particles' wettability.[34,35,36,37,38] Typically in a partitioning test, a known amount of test particles are dispersed in two immiscible liquid phases, normally water and a clear oil phase such as toluene or mineral oil. The mixture is well shaken and the particles' hydrophobicity is evaluated based on the amount of solids partitioned into the oil and water phase. The higher affinity to the oil phase indicates a higher hydrophobic level. This test is fast and easy to use, but the sensitivity is low. Particles that are of intermediate hydrophobicity would stabilize emulsions in which water droplets are trapped and the emulsion volume is case sensitive depending on the way the mixture was agitated. Normally, only a significant wettability difference between different samples could be detected by this method. Secondly, the wettability of the particles is influenced by the phase in which they are first dispersed. For example, It was noticed that solids dispersed in the oil phase first are more readily stay in the oil phase after partitioning, while those firstly dispersed in water are more difficult to enter the oil phase. This is probably due to change of wettability by the pre-adsorbed molecules of water or oil before the other phase is added.

2.4.2 Contact angle test by sessile droplet or captive bubbles

The contact angle test is the most commonly used method, which is quantitative and could reveal a relatively small wettability difference on smooth surfaces. The contact angle tests are adapted to evaluate the wettability of solids particles by compressing the solids samples into a compact solid disc with flat surface by either centrifugation[39] or compressing.[40,41,42] During a typical measurement, a water droplet is placed on the flat surface of the solid pellet and curvature of the droplet is imaged through a specially designed camera. The contact angle can be calculated by the aid of software that works together with the camera. This is called sessile drop contact angle measurement.[43, 44,45] Another type of contact angle test, the captive bubble contact angle measurement, is carried in water or a solvent environment and the contact angle is measured through the water phase by the curvature of an air bubble captured on the pellet surface.[39] The wettability evaluated by contact angle measurement is usually the average wettability of solid particles covered beneath the water droplet or air bubble. Thus, if the heterogeneous solid samples with a diverse range of wettability were used, it would result in large errors in the contact angle measurement.

2.4.3 Contact angle test by liquid penetrating

In this method, the contact angle between the probing liquid and solids can be calculated by measuring the penetration rate of the liquid into the compact solid pellet by Washburn equation [46]

$$\frac{h^2}{t} = \frac{r_{eff}^2}{8\eta l}\left[\frac{2\gamma_{lv}\cos\theta_p}{\gamma_{eff}} - \Delta\rho g h\right] \qquad (2\text{--}1)$$

Where η is the viscosity of the probing liquid, γ_{lv} is the surface tension of liquid, $\Delta\rho$ is the density different between the liquid and the solids, h is the penetration depth at a specific time, t, r_{eff} is the effective capillary radius, and θ_p is the

advancing contact angle. If $\Delta\rho gh$ can be ignored, the Washburn equation becomes:

$$\frac{h^2}{t} = \frac{r_{eff}\gamma_{lv}\cos\theta_p}{2\eta} \qquad\qquad (2\text{–}2)$$

Thus, the contact angle can be calculated by the penetration parameters (h and t) and the physical properties of the probing liquid (γ_{lv}, η).

Unlike the contact angle test, the liquid penetrating method does not require an equilibrium state to evaluate the wettability. Parameters needed in this method, such as h and t, are very easy to measure and thus, the water penetration time has a better sensitivity over contact angle measurement. However, the uniformity of the pore size in the substrates should be controlled, if comparison of the wettability of two substrates is needed.

2.4.4 Critical wetting surface tension measurement

A film flotation test, designed by researchers at UC Berkeley,[47,48] is used to evaluate the wettability of coal particles by their critical wetting surface tension. The critical wetting surface tension is defined as the highest surface tension the probing liquid could be, in order to completely wet the solid particle surface. In film flotation tests, sample particles are sprinkled onto the surface of probing liquid of different surface tension. Particles that sink through the surface would be considered wettable by the liquid, and those floated being non-wettable. A higher critical surface tension means less hydrophobic solids. This method is well suited to wettability evaluation for heterogeneous particles and has been used by many researchers[49,50] for wettability evaluation of coal or pigment particles. This method is also employed in our study, which will be discussed in details in Chapter 3.

2.5 Solvents impact on wettability

2.5.1 Solvent types

Naphtha

Naphtha is a mixture of a number of liquid hydrocarbons. In the oil sands industry, naphtha is a by-product from the petroleum refineries as an intermediate product from the distillation of hydrocarbons. Naphtha is commonly used as the diluent in the Syncrude bitumen froth-treatment process. Generally, there are two types of naphtha that are commonly referred as paraffinic naphtha and heavy naphtha. The paraffinic naphtha is normally less dense (low density) and has a higher paraffinic content. The heavier naphtha refers to the type that has higher content of naphthenes and aromatics, thus has higher density.

Toluene [51]

Toluene is clear water insoluble liquid with the molecular formula of C_7H_8 ($C_6H_5CH_3$) and its molecular structure includes an aromatic ring with one methyl group. The three alternating double bonds make toluene molecule having a delocalized electron that interacts with other ring structured organics. Thus, toluene has an affinity to almost all the components in bitumen, which makes bitumen completely soluble in toluene.

Heptane [52]

Heptane is straight-chain alkanes with the molecular formula of C_7H_{16}. Heptane is commonly used in laboratories as a non-polar solvent because of its symmetrical structure. Because of its zero dipole moment, heptane has a weak affinity for aromatics in bitumen, especially large hydrocarbon molecules with complex aromatic structures, such as asphaltene.

Heptol

Heptol is the mixture of heptane and toluene. Heptol can be formulated to have similar chemical properties as naphtha or to a solvent with a controllable paraffinic to

aromatic ratio. In our study, heptol refers to the 1:1 by volume mixture of heptane and toluene.

2.5.2 Solids wettability alteration by solvents

2.5.2.1 Effect of solvent surface tension and interfacial tension
According to Young's equation,

$$\cos \theta = \frac{\gamma_{sd} - \gamma_{sw}}{\gamma_{wd}} \qquad (2\text{--}3)$$

where γ_{sd}, γ_{sw} and γ_{wd} refer to the interfacial tension between solid and diluent (solvent) , solid and water and water and diluent, respectively. The contact angle θ (wettability) could be influenced by any of the three interfacial tensions in the above equation.
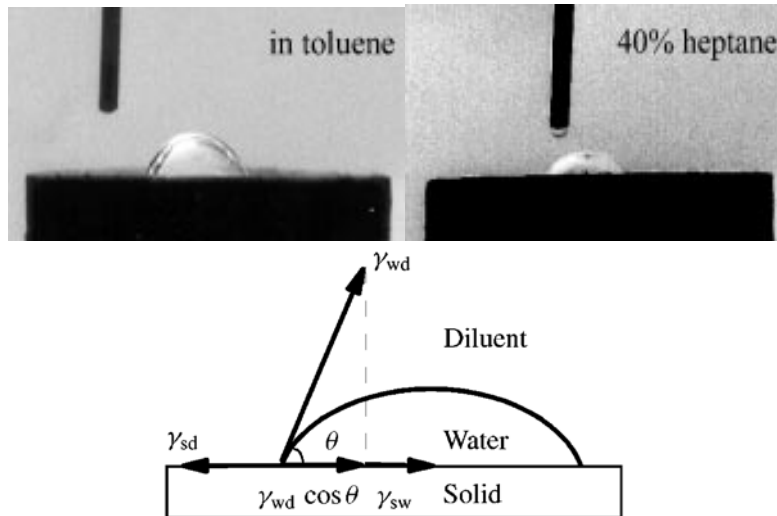
Figure 2-9. Influence of solvent interfacial tension on contact angle.[39]

By measuring the contact angle of water on a solid surface in different solvents, Chen et al. found that the contact angle is significantly smaller in a heptane-dominated solvent.[39] The interfacial tension measured by tensiometer indicated that the interfacial tension between solvents and water increases with the increase

of heptane volume percentage. Chen et al. suggested the decrease of interfacial tension as the major reason for the contact angle change in different solvents.[39]
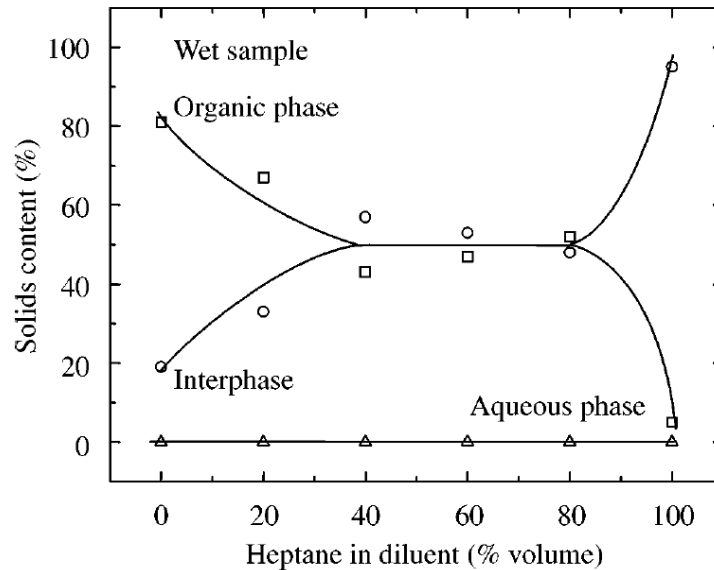
Figure 2-10. Solids partitioning behavior when different solvents used.[39]

Their contact angle results were confirmed by partitioning of the solids between the organic and aqueous phase. As the volume percentage of heptane is increased in the diluent, more solids were found at the inter-phase rather than in the hydrocarbon phase, indicating a decreased hydrophobicity.

2.5.2.2 The effect of solvent washing

It is well accepted that the wettability of solids in oil sands is directly influenced by the adsorbed hydrocarbons on the solid surface.[15,16] Depending on the solvent polarity and solubility, the hydrocarbon amount could be changed by different extent of solvent treatment. Some researchers had studied the impact of solvent washing on the wettability of solids. Chen et al. studied the wettability of froth solids after being washed by toluene and heptane.[39] They found that toluene washing made the solid surface far more hydrophilic than heptane washing. This is due to toluene's better hydrocarbon-dissolving power over heptane.

Dan Vu et al.[53] have reported a sequential solvent washing process to remove the surface hydrocarbons. They found that toluene, when used solely to wash solids

with a coated hydrocarbon on their surface, was not able to wash off all the organics. After the solids were washed by toluene until the supernatant became colorless, a subsequent methanol washing on the solids made the supernatant dark again. They also found that the followed methanol treatment made the solids cleaner than the toluene treated ones.

2.6 Objective of this work

Though wettability of solids is found to be strongly related to the stability of water in oil emulsions and hence bitumen froth treatment proficiency, little has been reported on the impact of solvents on wettability. The conditions using extensive fresh solvents washing to study their impact on solids wettability[39,53] are different from the reality encountered in a bitumen froth treatment process where the removal of hydrocarbons from a surface by solvents and adsorption of hydrocarbons onto the solid surface in solvents occur at the same time.

In this study, toluene, heptane and their mixtures were used to study the impact of solvents properties on solids wettability. Both hydrocarbon removal and adsorption are considered to shed light on the interactions between hydrocarbons, solvents and solids in a froth treatment environment. The understandings to these interactions are important in explaining the different froth treatment performances observed in different solvent-treatment environments.

CHAPTER 3 MODEL SOLIDS SYSTEMS

3.1 Introduction

To study the impact of solvents on the wettability of solids in complex system, such as diluted bitumen froth, it is always easier to begin with model systems, as the mechanism could be easier revealed by identifying the changing parameters. In this study, four types of commonly seen froth solids were used as model solids. They were kaolinite, illite, silica and siderite. To study the effect of solvents on the wettability of solids, two types of solvents and their mixture were used in this study, namely: toluene (aromatic), heptanes (paraffinic) and heptol (1:1 toluene/heptanes mixture by volume)

The wettability of solids in the diluted froth was believed to be a combined result of both the original wettability of minerals and the absorbed surface hydrocarbons. A schematic diagram is given in figure 3-1 to illustrate by what ways the solvent can impact the wettability of froth solids-type. While the solvents are not likely to be able to change the mineral surface wettability, they probably can:

a. impact the partitioning behavior of minerals, by having different affinities for different minerals , and,
b. affect the hydrocarbon's interaction with the solid surface, which includes adsorption and removal of hydrocarbons by solvent washing.
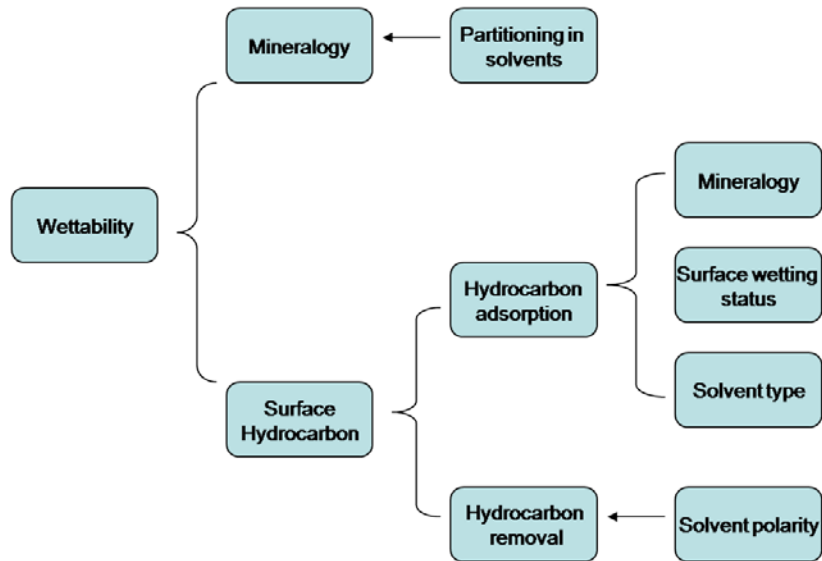
Figure 3-1. Relationship tree of factors influencing the wettability of froth solids.

In the model system study, we designed several experiments to explore the relationship illustrated in figure 1-1.

3.2 Techniques and facilites

The next several sections will provide a description of the techniques and facilities used in this model study. A mastersizer laser-diffraction apparatus was employed to measure the particle size distribution of the mineral powders and a Drop Shape Analyzer (DSA) was used to characterize the solids on its wettability. The techniques used include contact angle measurement and water penetration time measurement, which will be discussed in details in the following section.

3.2.1. Particle size distribution measurement

The particle size distribution of the model minerals was measured with a Malvern Mastersizer 2000 particle analyzer manufactured by the Malvern Instruments Ltd., UK. The particle size measurement of this apparatus is based on the principle of laser ensemble light scattering. The laser beam generated from the analyzer is illuminated though water with suspended sample particles and based on the Mie scattering theory[54], the particle size is inversely proportional to the angle of

scattering beam. The calculated particle distribution was calculated following the Mie scattering model and the percentage of particles sized within the resolution range 0.1 micron to 1000 micron were reported , as well as the D(10), D(50) and D(90) percentile sizes.

The accuracy of the size distribution measurement is largely dependent on the dispersion condition of the particles in water. The system employs a chamber in which the water suspension was kept agitated during the course of the measurement. To achieve a well dispersed suspension, 3-4 drops of sodium-silicate solution were added into the mixture of 0.2 g sample particles in 10ml de-ionized water. The suspension was then shaken vigorously by hand, followed by a 30-minutes ultra-sonic bath treatment. The well-dispersed suspension appeared homogeneous and the particle size distribution was measured quickly to avoid agglomeration.

The results of the particle size distributions of the minerals were shown in figure 3-2 and the percentile sizes for each mineral were shown in table 3-1.
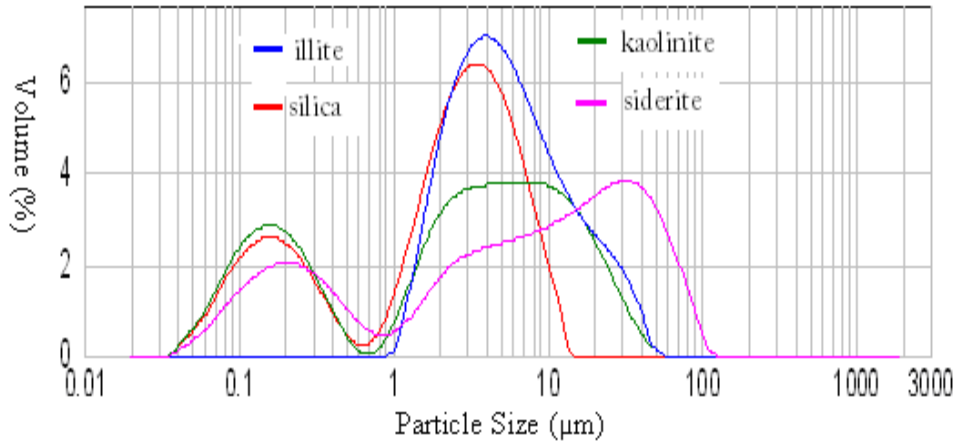
Figure 3-2. Particle size distribution of the model minerals.

Table 3-1. D(0.1), D (0.5) and D(0.9) of model minerals.

Mineral	D(0.1) μm	D(0.5) μm	D(0.9) μm
Silica	0.13	2.4	6.9
Kaolinite	0.12	3.2	17.6
Illite	2.0	5.2	19.8
Siderite	0.17	7.7	48.2

The particle-size distribution measurement showed a bi-modal distribution for each mineral. The percentage of solids smaller than 1 micron is similar for all the mineral samples. The results in Table 3-1 showed that for each mineral sample, up to 90% of the volume has sizes within 44 microns, suggesting the majority of the solids used are fines (< 44 micron) , among which siderite has slightly larger D50 size. The high repeatability of the results suggests that the particles were effectively dispersed during the particle-size distribution measurements.

3.2.2 Wettability evaluation techniques and equipment.

The evaluation of the wettability of solids was achieved by two experimental techniques, namely the contact angle (CA) measurement and Water Drop Penetration Time (WDPT) measurement. The afore-mentioned two techniques will be discussed in details in a subsequent section.

3.2.2.1 Preparation of compact solids discs

Figure 3-3. The smooth surface of a compact solid disc used in this study.

Before evaluating the wettability by CA, the solids have to be compacted into discs with smooth surfaces. A manual hydraulic press (Enerpac JH-5) and a die were used to prepare these pellets. The die has a diameter of 22.5 mm and a smooth surface, which was in direct contact with the solids during the pressing. Under room temperature, 5 grams of solids were carefully weighed and transferred into the die, on which a pressing force of 9000 psi was loaded for 4 minutes before the sample disc was carefully removed. The solid disc prepared as such has a flat and smooth finish as suggested by its reflectivity (Figure 3-3) and was used immediately for water drop penetration time measurements.

3.2.2.2 Contact angle measurement

The contact angle (CA) measurement is one of the most easy to adopt and commonly used techniques for wettability evaluation. The CA measurement uses the shape of a liquid droplet resting on a solid surface to describe how wettable the solid is to the probing liquid.
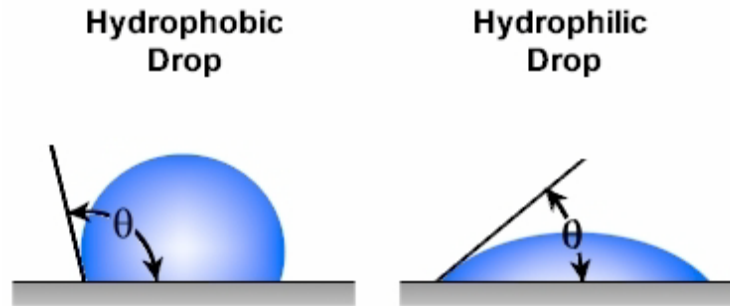
Figure 3-4. Schematic view of water droplet on a hydrophobic surface and hydrophilic surface.

The contact angle is the angle formed between the liquid/solid interface and the liquid/vapor interface. It could be determined by the adhesive-force between the liquid and solid surface and cohesive-force within the liquid. While the adhesive force makes the liquid spread on the solid, the cohesive force gives the liquid droplet tendency to sphere up. The interfacial work of adhesion W_A could be expressed as

$$W_A = \gamma_s + \gamma_l - \gamma_{sl} \tag{3–1}$$

, where γ_s is the interfacial tension between solid surface and gas, γ_l is the surface tension of liquid and γ_{sl} is the interfacial tension between solid and liquid. The work of cohesion of the two contact surfaces W_C could be expressed as

$$W_C = 2\gamma_l \tag{3–2}$$

The spreading coefficient S, which describes the minimum energy needed to spread the liquid over the solid surface could be expressed as:

$$S = W_A - W_C = \gamma_s - \gamma_l - \gamma_{sl} \tag{3–3}$$

The spreading condition requires the work of adhesion to be larger than the work of cohesion, thus, S greater than zero.

As shown in figure 3-4, a water droplet on a hydrophobic surface tends to have higher contact angle than when on a hydrophilic surface. The shape of a droplet on a solid surface is dependent on the relative tensions of the system interfaces. On a simplified ideal solid surface with perfect smoothness rigidity and chemical homogeneity, the contact angle could be calculated following the Young's equation:

$$\gamma_s = \gamma_{sl} + \gamma_l \cos\theta \tag{3–4}$$

Thus,

$$\cos\theta = \frac{\gamma_s - \gamma_{sl}}{\gamma_l} = 1 + \frac{S}{\gamma_l} \tag{3–5}$$

Thus, the contact angle is good indicator for the spreading coefficient, and the ability of the liquid to wet the solid surface.

3.2.2.3 Water drop penetration time test

Another test called the 'Water Drop Penetration Time' (WDPT) was also used for the evaluation of the solids wettability. The WDPT is the time required for a known volume of water droplet to completely penetrate the solid disc. This value indicates the water repellent nature of the solids, and reveals the accumulative hydrophobicity of solids covered beneath the water droplet. For each experiment, a calibrated dosing-syringe was used to control the volume of the water droplet and the penetration of water into the sample pellet was recorded as a video clip at a frame-rate of 200ms/frame. The time for the water droplet (40µL) to infiltrate the compressed solids surface was calculated by software at a resolution of 200ms. The WDPT results are partially dependent on the pore size of the solids in the

compressed disc, as they provide different levels of capillary forces. Thus, only particles with size smaller than 45 microns were used in this test.

3.2.2.4 Drop shape analyzer

(a)

(b)

(c)
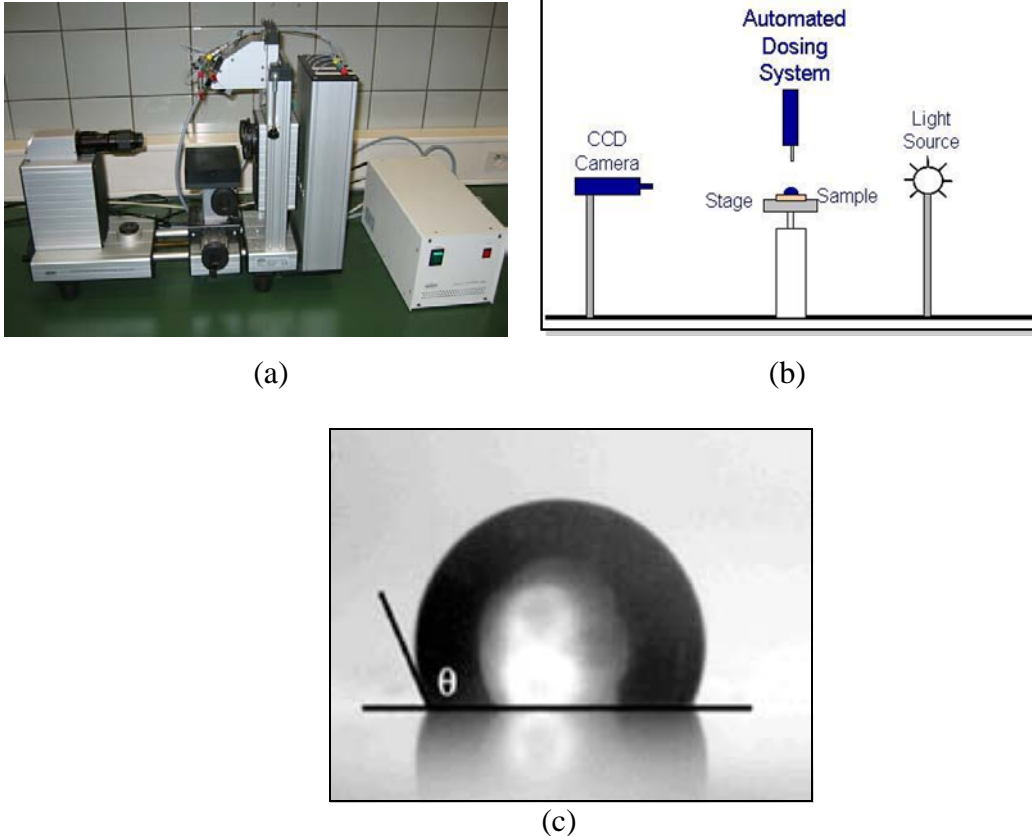
Figure 3-5. Drop Shape Analyzer.
(a). Picture of the Drop Shape Analyzer.   (b). Schematic view of the Drop Shape Analyzer. (c). Droplet being analyzed

Both the CA and WDPT measurements were carried out on the Drop Shape Analyzer system, manufactured by KRÜSS inc., Germany. The photograph of the system and a schematic view were shown in figure 3-5 a. and b. respectively. The setup includes an automatic dosing system for droplet volume control, a six-direction removable platform to support the sample surface, a light source to illuminate the sample stage and a CCD camera, which captures the shape of the droplets. The shape of the droplet was magnified on a computer screen as shown in figure 3-5c and the image sharpness can be adjusted through the brightness of the light source.

The contact angles are measured by fitting a mathematical expression to the shape of the drop and then calculating the slope of the tangent to the drop at the liquid-solid-vapor (LSV) interface. The video clip of the droplet penetrating the solid pellet was recorded by the software and the WDPT was recorded as the time a droplet took to completely penetrate into the solid disc. The sample surfaces used in this study include compact solids discs and flat surface of contaminated silica wafers. The contact angle and WDPT values obtained by DSA are heavily dependent on the position of the interface shown in figure 3-5c, which is user-identified. Thus, correctly determining the interface position is crucial in this experiment. In our experiments, the interface was always chosen at the symmetrical line between the image of the droplet and that of its reflection on the testing surface. When the contact angle is close to 90°, the interface line would be difficult to determine as the curvature of the droplets and its reflection would appear continuous.

3.3 Minerals partitioning test

3.3.1 Experiment

To observe different minerals partitioning behaviour between different solvents and water, the experimental set-up shown schematically in figure 3-6 was used.
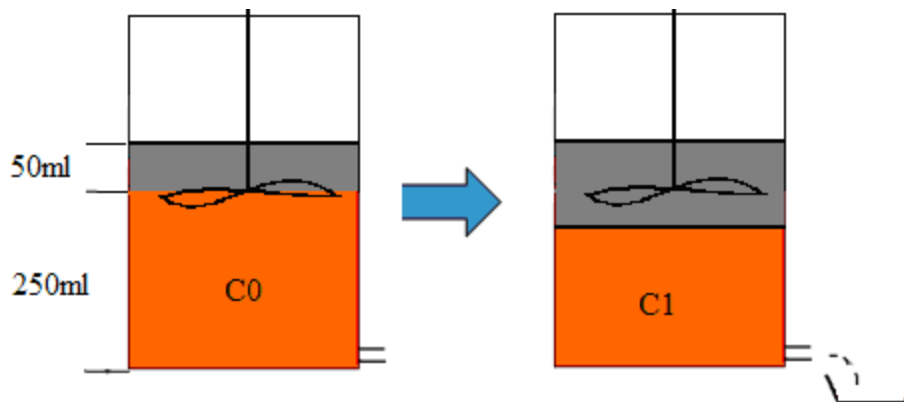
Figure 3-6. Procedure for mineral partitioning test.

A 500ml glass cylinder was constructed with volume marks on its wall. A small outlet was attached to one side near the bottom of the cylinder to allow the lower phase in the cylinder to be drained out. In each test, 2.5g of solids were dispersed well into 250 ml de-ionized water by an impeller inside the cylinder, followed by the placement of 50ml of solvent-diluted bitumen on the top. The solvents used for dilution was either heptane or toluene. After dilution, the diluted bitumen phase was referred as Tol-Dil-Bit or Hep-Dil-Bit, corresponding to toluene and heptane as diluent, respectively. With an impeller positioned at the hydrocarbon-water interface, when the impeller was rotated at 700rpm, the hydrocarbon phase was broken into small oil droplets dispersed in the lower aqueous phase. Hydrophobic solid particles in the aqueous phase were picked up by the dispersed oil droplets and they reported to the top oil phase after stopping the impeller rotation. The partitioning of the solids was then characterized by the amount of solids 'picked up' and the volume of oil-in-water emulsion formed.

The volume of the oil in water emulsion formed after the partitioning was recorded by reading the volume scale on the vessel prior to any drainage. The aqueous layer was then drained through the bottom vessel outlet and the amount of solids left in the water phase was collected by centrifuging the collected aqueous suspension at 200,000g-force, followed by a drying process in a vacuum oven at 80°C overnight. The amount of solids 'picked up' by the oil phase was calculated from the difference between the total solids added and the amount left in the aqueous phase after partitioning.

3.3.2 Results and discussion

The volumes of the aqueous and oil phase formed are shown by bar charts in figure 3-7. The oil phase here refers to the total phase of diluted bitumen phase and oil in water emulsion phase. The line at 250ml indicates the position of the original interface between the water and diluted bitumen before the partitioning tests, i.e. the 'start line' was at 250 ml of water suspension and 50ml diluted bitumen for each system. After the partitioning, for all the mineral/Dil-Bit

combinations, a varying amount of oil in water emulsion was observed. The siderite mineral appears to be the most significant in emulsification of the oil phase, measured by the largest emulsion volume. As solids of suitable wettability are believed to be an effective emulsion stabilizing agent, this observation suggests that siderite mineral has the strongest affinity to the hydrocarbons and hence being biwettable.

The difference in partitioning behaviors between illite and kaolinite is not as significant although a kaolinite system generated slightly more emulsion than illite.

Regarding to the differences due to types of solvents, for the siderite, more emulsion was formed in a heptane diluted system and for the illite mineral, the emulsion volume formed in a heptane diluted system was slightly less than that in the toluene diluted system. The difference for the kaolinite system is not significant. These trends were reproducible.

.
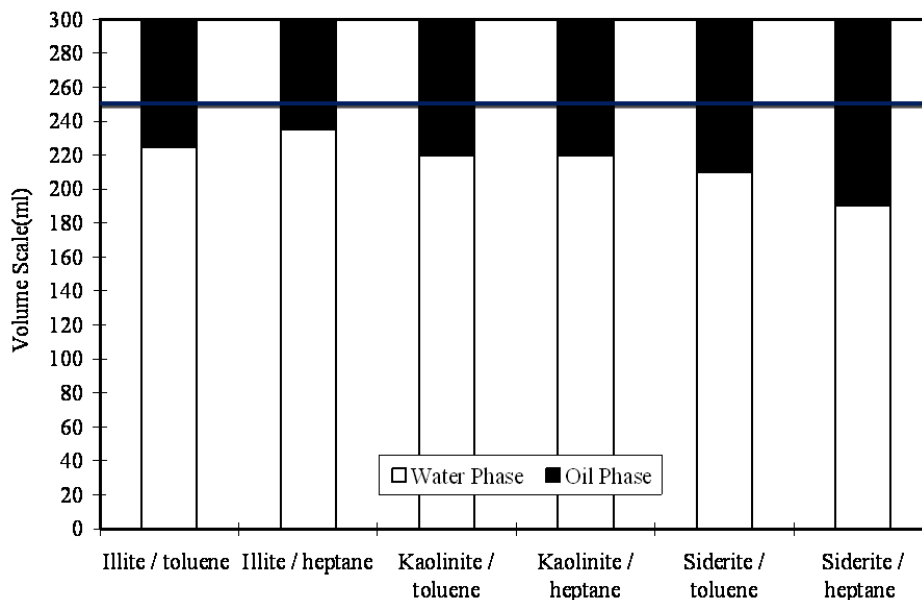
Figure 3-7. Volume of emulsion formed in oil phase after partitioning tests.
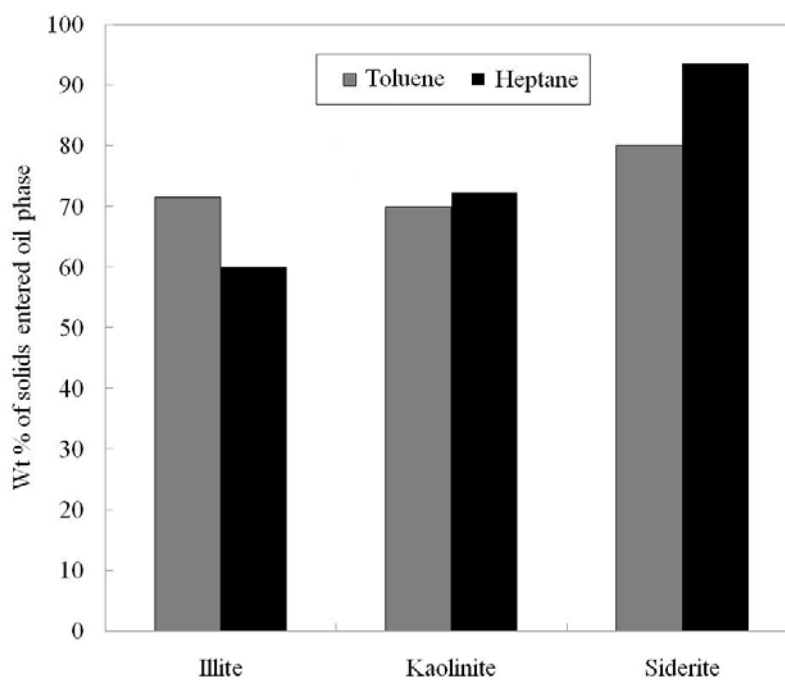
Figure 3-8. Percentage of solid particles reported to the oil phase after partitioning.

Figure 3-8 shows the percentage of solids that actually entered into the hydrocarbon layer after partitioning. The trend corresponds well with the amount of water in oil emulsion formed. It is interesting to note that even for hydrophilic

solids such as kaolinite and illite, the majority of the solids (>60%) was picked up into the hydrocarbon layer. This is probably due to the surface contamination and wettability alternation during the partitioning process. The siderite showed a selectivity for the heptane diluted system and illite mineral showed a selectivity for the toluene diluted system. These results indicated that for different minerals, they did show different partition behaviors as in different solvents. The results suggest the possibility that certain solvents could cause more severe contamination of solids than other solvents used for diluting bitumen. The mineralogy might determine interactions of solids with organics in bitumen which in turn determine the wettability of solids leading to preferred partition in organic phases.

3.4 Model solids contamination test

In section 3.3, it was found that different minerals partitioning behavior could be different as different solvents are used to dilute the bitumen phase. In this section, we investigate the minerals vulnerability to wettability alteration. In a froth treatment process, the wettability alteration would happen when the hydrocarbon molecules adsorb onto the solids surface, or when the already adsorbed molecules in oil sands have been removed by solvents dissolution. The following experiments were designed to study the factors that could change the wettability of solids.

3.4.1 Pre-wetting conditions of solids.

When considering the adsorption of hydrocarbons onto a solid surface, the original surface wetting condition of the solids might be of importance as any "water film" on the solids surface would serve as a shield to keep the solids surface away from the hydrocarbon molecules or as a binder for the surfactants to adsorb onto the surface.

In order to study how the adsorbed surface water might play a role in solids'
contamination by hydrocarbons, the surface wetting condition of model solids was
altered prior to the partitioning tests. Three batches of each mineral type were
prepared by either (1) drying in a vacuum oven, (2) wetting in water vapor
environment or (3) used as received.

The drying process was carried out in a vacuum oven at 80°C overnight. The
water wetting procedure was carried out in a filter cone above boiling water. The
setup is shown schematically in figure 3-9.
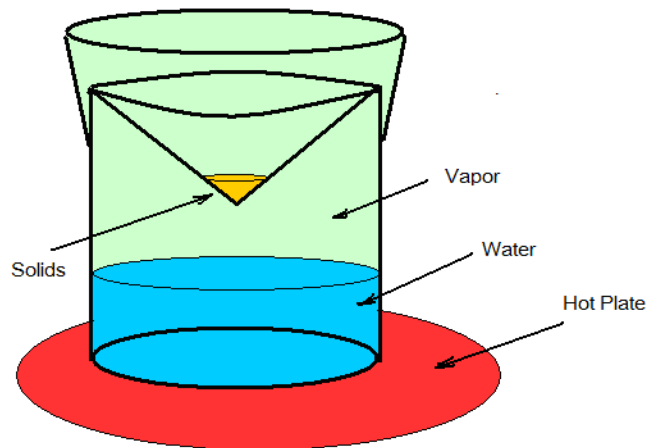
Figure 3-9. Experimental setup for solids pre-wetting.

The filter cone with solids was placed on the top of a beaker with boiling water.
The water vapor comes through the filter paper and condenses on the surface of
testing solids to form a water film. The exposure time was controlled at 10
minutes.

3.4.2 Experiment–mineral contamination test

5g of each solids sample, after pre-treatment where applicable, was then dispersed
into 120ml diluted bitumen solution with bitumen concentration of 10g/L. After
shaking for 15 hours, the solids were collected using centrifugation and washed
with de-ionized water to remove any free hydrocarbon trapped in the voids of the
solids. The free oil that was not strongly adsorbed would be removed by water

washing and accumulated to form a black hydrocarbon layer on the top of the aqueous phase after centrifugation at 20,000g-force. This washing process was repeated until no free oil can be washed off as indicated by no visible oil on the top of the water phase after centrifugation. The whole procedure is shown schematically in figure 3-10.
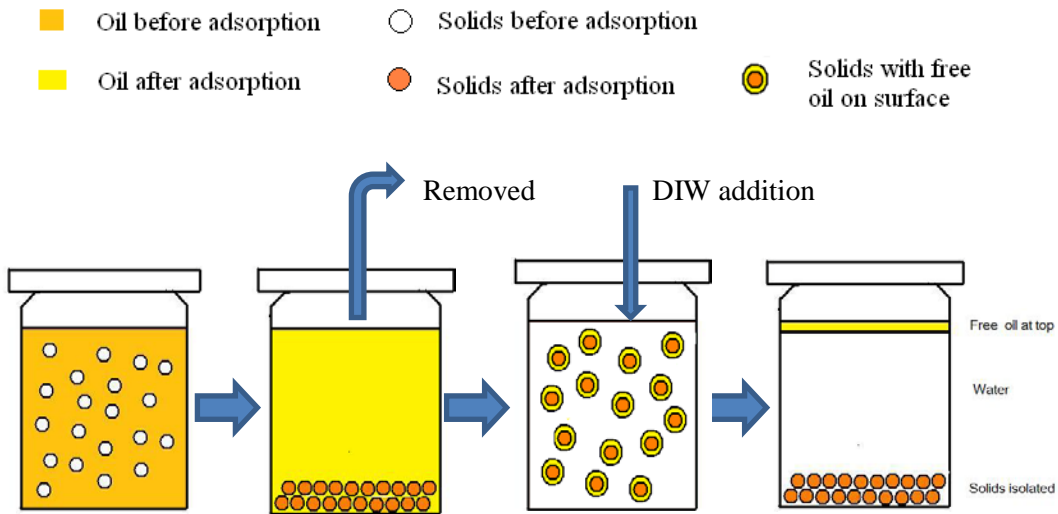
Figure 3-10. Experimental procedure for solids contamination tests.

The solids extracted as described above, were compacted into a solid disc by a manual hydraulic press ((Enerpac JH-5) and a die with a diameter of 22.5mm as described in 3.2.2.1. They were then used immediately for water drop penetration time measurements.

3.4.3 Results–mineral wettability after contamination
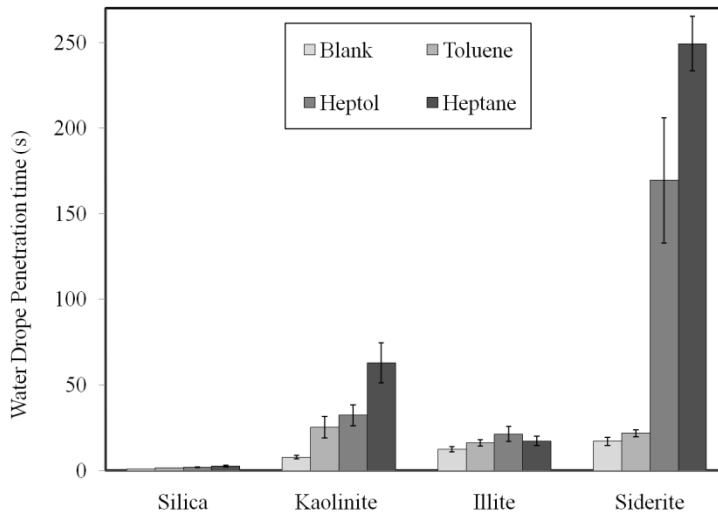
Figure 3-11. Water Drop Penetration Time results for contaminated solids without pre- treatments.

The observed water penetration time on the contaminated solids without pre-wetting condition treatment showed some variation. The results revealed that both the solids mineralogy and the solvent composition played a role in the wettability alteration. The column with the lightest color in figure 3-11 shows the penetration time for the untreated solid discs (Blank). The kaolinite, illite and siderite discs used here showed a very similar wettability prior to hydrocarbon exposure. The WDPT on these discs are around 7s. The silica disc however was found to be more hydrophilic than the other three. It has a water penetration time of around 2s, indicating a highly hydrophilic nature. The hydrocarbon contamination made all solids more hydrophobic, as indicated by a longer water droplet penetration time. The extent of wettability alteration depends on the composition of solvent. For kaolinite and siderite, the WDPT increased with increasing heptane content in the solvents. Compared with kaolinite, a more significant increase in wettability was seen for siderite, in which case the WDPT increased drastically to greater than 250s with the treatment in hetpane diluted bitumen solution. The silica and illite, however, did not show a significant change in wettability when treated with bitumen in different solvents. This corresponds to our solids partitioning tests that

39

illite was found to have very similar partitioning behavior in hetpane diluted bitumen and toluene diluted bitumen.
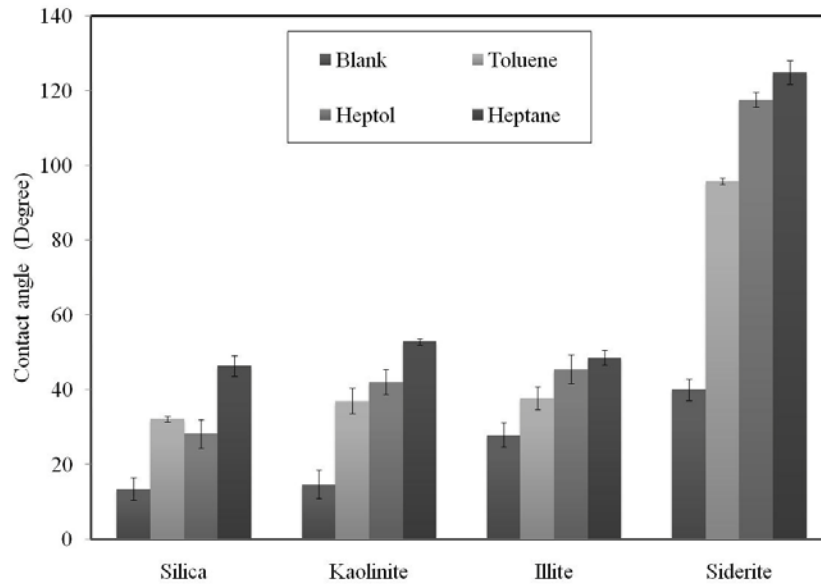
Figure 3-12. Initial contact angle on the contaminated solid discs.

To support the WDPT results, the contact angle results suggested that a more hydrophobic surface normally has larger water contact angle and longer WDPT. Depending on the solvents composition, the contact angle on the contaminated siderite disc varied from 97° to 125°. These values are much higher than those found on other mineral discs, which varied in the range of 30°-50°. This indicated a much more hydrophobic nature of the siderite minerals after contamination. Generally, the contact angle results corresponded very well with WDPT results. One exception is that, even though the silica discs have very similar contact angle value as that of kaolinite and illite discs, the WDPT was significantly smaller. This may indicate that WDPT test is more sensitive than contact angle measurements.
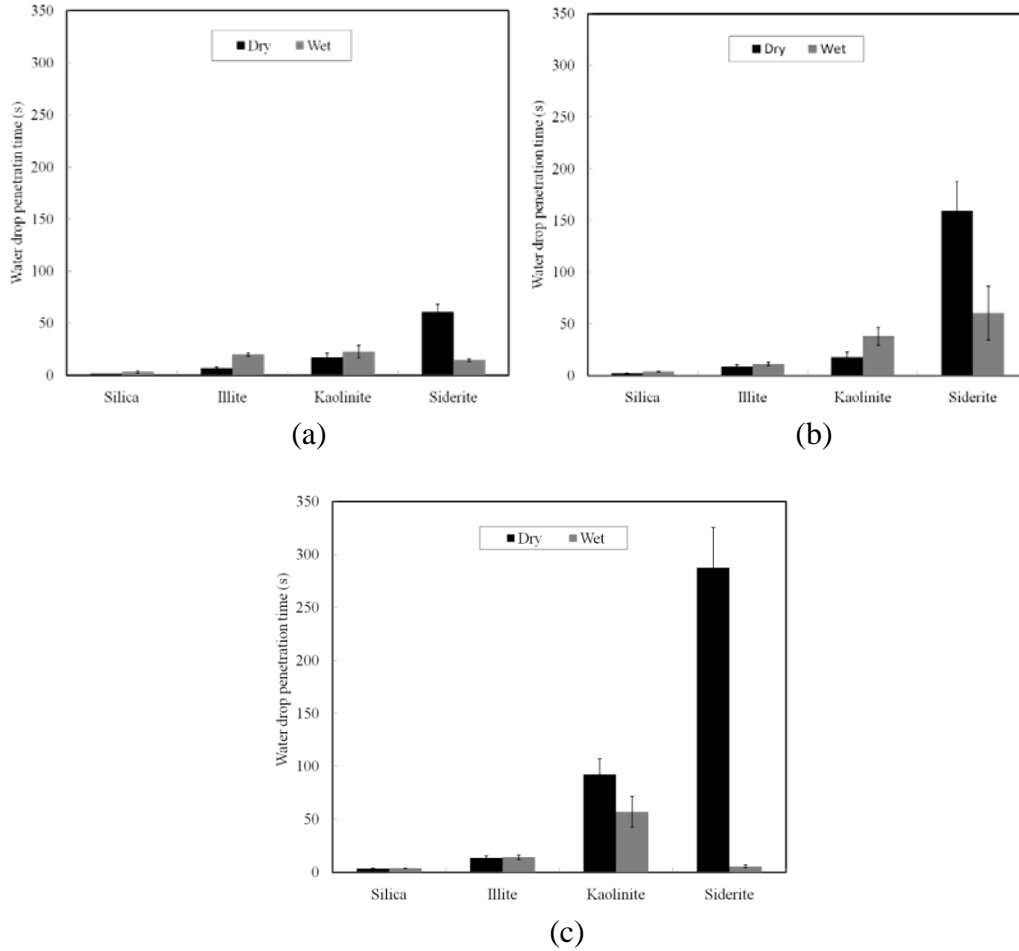
Figure 3-13. Effect of original wetting condition on wettability of clays by hydrocarbon- contamination (a) in toluene diluted system, (b) in heptol diluted system, (c) in heptane diluted system.

Figure 3-13 shows the effect of surface pre-wetting condition on the wettability change by hydrocarbon contamination of clay surfaces. It is interesting to note that for silica and illite minerals, the surface wettability does not respond to the change of solvent composition. The drying or steaming does not seem to change surface interaction of these clays with bitumen components in various solvents thereby exhibiting a similar WDPT. The original wetting state of kaolinite does not seem to affect hydrocarbon contamination in toluene and heptol diluted bitumen solutions. However, a noticeable decrease in WDPT was observed when the original surface was pre-wetted prior to its exposure to the heptane diluted bitumen solution. A much more significant decrease in WDPT was observed when siderite was treated with water vapor prior to its exposure to solvent-diluted

solutions. It is evident that strong hydration of siderite greatly hindered its interaction with bitumen components in all the solvents, with the change in heptane being the most significant, as shown in figure 13-3c.

3.4.4 Mechanism discussion - surface precipitation caused by poor solvents

The largest wettability alteration with the bitumen in paraffinic solvent solution could be explained by poor solubility of the asphaltene components in paraffinics.

(a)   (b)
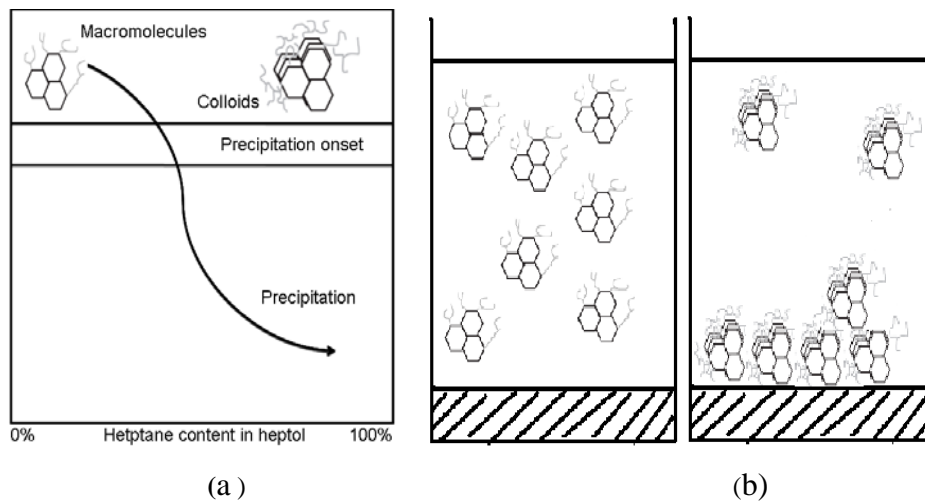
Figure 3-14. Asphaltene surface precipitation in poor solvents.
(a). stability decreases with increase of heptane percentage.(b). Possible stacking mechanism.

In poor solvents, even before the precipitation is triggered, the asphaltene molecules could coagulate to form aggregates on solid surfaces to lower the energy state of the system, which was first proposed by Buckley and her colleagues [55,56,57]. When using asphaltene solutions to rinse the solid surface, they found that asphaltenes dissolved in poor solvents rendered the surface to be much more oil-wet. They proposed that the contribution of this colloidal mechanism to the wettability alteration is dependent on the quality of solvents and the level of asphaltene aggregation. They proposed that the onset of the asphaltene precipitation could be predicted using the refractive index of the crude oil as an indicator of the intermolecular forces which determines the solvency.[58]

3.4.5 Mechanism Discussion -minerals interaction with hydrocarbons

The difference between the adsorption behaviors of kaolinite and illite may be explained by their crystal structure difference.

3.4.5.1 The structure of kaolinite and illite
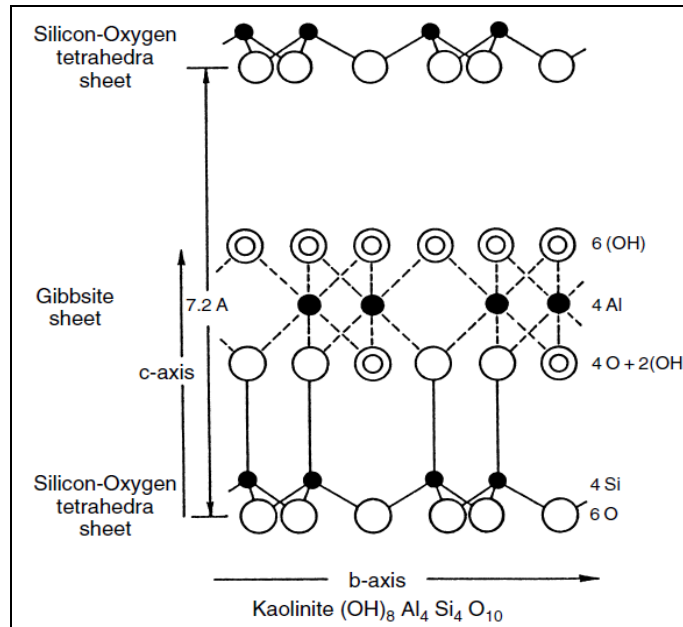
Figure 3-15. Structure of kaolinite.

The chemical formula of kaolinite is $Al_4Si_4O_{10}(OH)_8$. Its crystalline structure consists of two layers that a silicon-oxygen tetrahedral layer joints the alumina octahedral layer alternatively.[59] The 1:1 sheet structure composed of SiO_4 tetrahedral sheets and $Al(O,OH)_6$ octahedral sheets are created from planes, which are occupied following the sequence of

$$Si_4 - O_6 - (OH)_6 - Al_4 - O_4, (OH)_2$$
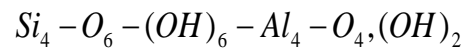
A model of its structure was shown in figure 3-15.
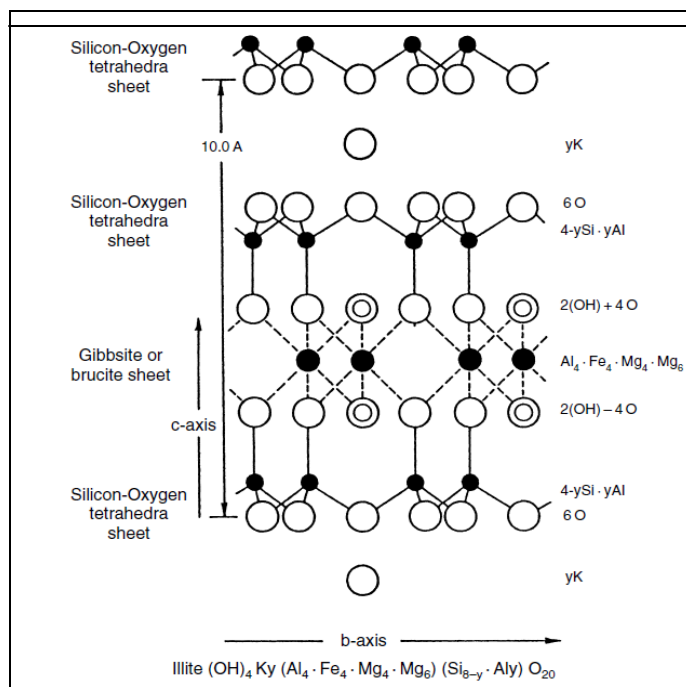
Figure 3-16 Structure of Illite.

Illite has a typical chemical formula of

$$(OH)_4 K_y (Al_4 Fe_4 Mg_4 Mg_6)(Si_{6-y} Al_y)O_{20}$$
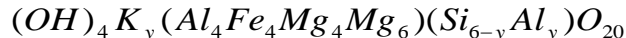
with ion substitutions. Its crystalline structure involves a tetrahedral-octahedral-tetrahedral (TOT) formula, that the octahedral Gibbsite-sheet is sandwiched by two silicon oxygen tetrahedral sheets. The elemental structures are linked by interface that is occupied by potassium ions. The interface is small and would prevent the water molecules from entering, thus, illite is non-expanding in nature.[60] A model of its structure is shown in figure 3-16.

3.4.5.2 Functional groups on the surface interacting with oil molecules

From mineralogical perspectives, both of kaolinite and illite are of layered structures with kaolinite having two-layer structure while illite having three-layer structure. The interaction force between the inter-layers is much weaker than that within the layer. This leads to an interesting supposition that the wettability would be related to the nature of cleavage plane.

44

The cleavage of kaolinite leads to an Al-OH plane and a Si-O plane while the cleavage of illite leads to two Si-O planes. On the broken edges, kaolinite features 1:1 Si/Al molar ratio in contrast to 2:1 molar ratio for illite. It is clear that illite would have less exposed Al-OH functional groups on their surfaces. The difference in the interactions of hydrocarbon molecules with clay solid surface would possibly be linked to their interactions with surface Al-OH and Si-O functional groups.

Several researchers[61,62] reported results in support of this supposition. Using Fourier transform infrared spectroscopy (FTIR) and X-ray adsorption spectroscope (XAS), the adsorption of asphaltenes onto clays has been investigated by Bantignies et al.[61] They showed that only Al-OH functional groups would interact with asphaltene molecules. The XAS analysis revealed that local environment of Al in kaolinite is changed during adsorption but the Si environment remained insensitive in kaolinite. They also found that the adsorption of asphaltene on illite did not change the chemical environment of the Al or Si in illite.

Saada et al.[63] compared the hydrophobicity of kaolinite and illite by adsorption tests carried in water vapor and asphaltene solutions. They found that a large amount of asphaltene adsorbed on kaolinite while illite showed more affinity to water vapor. They also found that the adsorption capacity of water on clays increased significantly while the adsorption capacity of asphaltene decreased when the clays were exchanged with Na^+ cations. This finding suggests that the high cation exchange capacity (CEC) of illite also plays an important role in its less vulnerability to hydrocarbon contamination.

3.4.6 Mechanism discussion- effect of the water film on the solid surface

These results indicated that whether water film on the surface would serve as protective shield or not depends on the nature of the solid surface and the adsorption medium.

(a)

(b)

Toluene as solvent

Asphaltenes

Asphaltene molecule

Solids

Surfactants

Water film
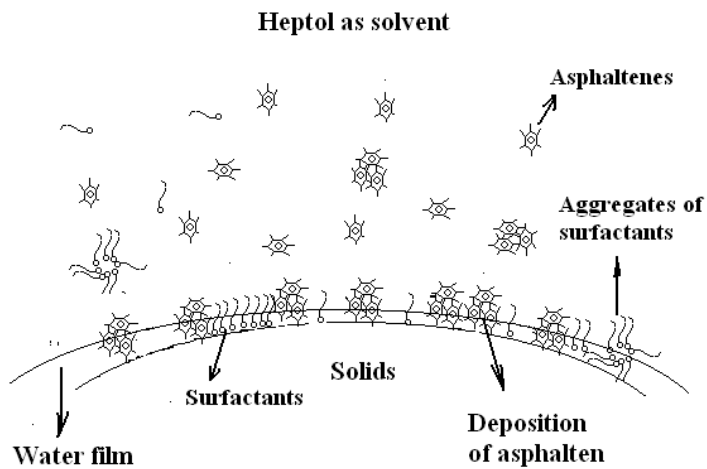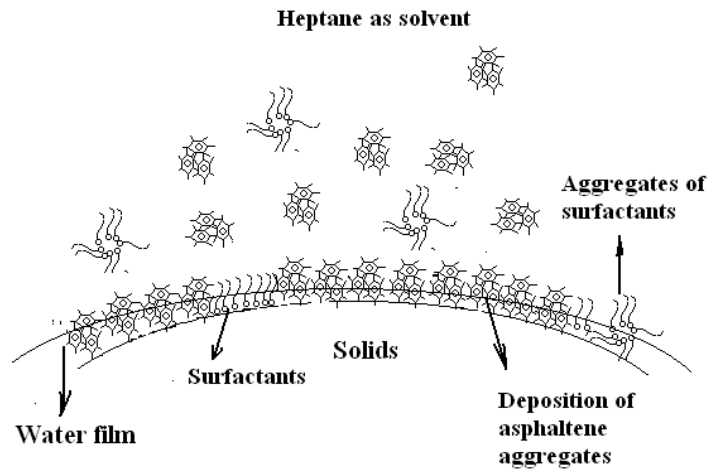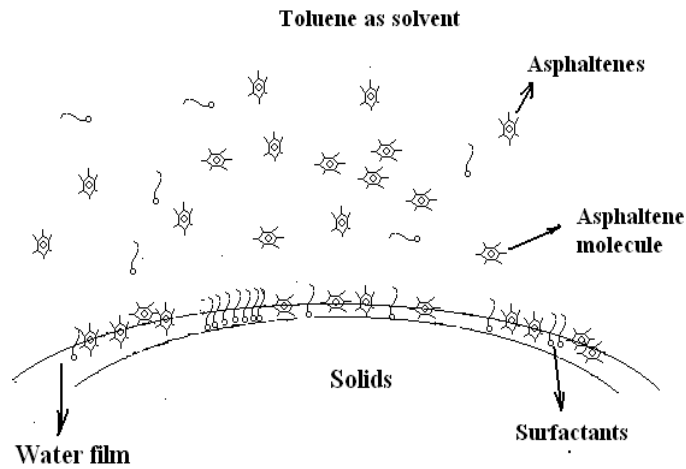
(c)

Figure 3-17. Interaction between surface-active components and an interface when the solid surface is pre-wetted. (a) heptane as solvent, (b) heptol as solvent. (c) toluene as solvent.

Upon exposure with water vapor, strong interaction of surface –OH group with water by hydrogen bonding would lead to significant water condensation. Whether the asphaltene would firmly adsorb onto the surface depends on the state of the water film on the solid surface. The water film is believed to have two functions, serving as a bridge, which attracts more surface-active components to the oil/water interface from the diluted bitumen, and as a shield, which keeps the hydrocarbon away from adsorbing onto the solid surface. The shielding effect of water film on wettability alteration is not significant when toluene or heptol were used as solvents, as shown by more hydrophobic surfaces after contaminating a water pre-wetted surface. The water film appears to provide a reservoir for polar groups of less aggregated surface-active components to interact with solids while keeping hydrocarbon tails in the solvent, leading to a more hydrophobic surface as it was observed that a pre-wetted surface treated in toluene- or heptol-diluted bitumen are generally more hydrophobic (with siderite as an exception). This indicates that the contamination was promoted to a water pre-wetted surface. The difference of contamination in heptol and toluene is mainly due to the different driving force for surface-active components to move onto the solid surface. The

47

trend is consistent with the results for dry solids. Due to a less polar nature of heptol than toluene, as anticipated, the surfactant-like components appear to be more surface-active. As a result, more hydrocarbons are driven onto the surface in heptol than in toluene, leading to a more hydrophobic surface after exposure to bitumen solution. The situation in heptane is more complicated. On one hand, the driving force for the asphaltene to move onto the interface is high due to the unfavorable energy state of asphaltene in the non-polar solvent, leading to an easier precipitation of aggregated asphaltene (figure 13-17a). On the other hand, the aggregates themselves are less surface-active due to shielding of the surface-active polar groups from non-polar solvent. The water film would also be more associated with solids in heptane and the aggregates will then have to interact with solids across a water film. This is probably the reason that in the heptane diluted solution, contamination on a pre-wetted surface is more difficult. Kaolinite and siderite all showed a reduced contamination in heptane diluted bitumen with water pre-wetted surface.

With regard to siderite, it appears that the untreated - siderite surfaces are capable of forming strong hydrogen bounding with the surface-active components of bitumen due to the presence of surface –OH groups, leading to severe hydrocarbon contamination when dry siderite was treated. Although the presence of water on siderite would lead to adsorption of surface-active components of bitumen at oil/water interface, the presence of surface –OH groups also make the water film stable in heptane dominated solvents. Thus, the weak binding through a water layer makes adsorbed hydrocarbons vulnerable to subsequent solvent washing, leading to reduced contamination.

3.5   Silica wafer contamination tests

In section 3.4, we had studied the impact of mineralogy and original surface wetting condition on the oil contamination for the solids. In this section, we use the silica wafers to study the impact of the original solids surface wettability on the hydrocarbon-contamination. Silica wafers were chosen as the substrate here as silica is one of the most abundant minerals in the froth and the flatness and smoothness of the wafer surface would provide a perfect substrate for the contact angle measurement.

3.5.1 Surface wettability.

The hydrophobicity of silica wafers surface was changed by baking at elevated temperature before been subjected to contamination tests. Silica wafers with diameter of 10 cm purchased from the Nanofabrication laboratory at University of Alberta were cut into 1.5cm x 1.5 cm chips. The chips were then treated as follows.

A. **Hydrophilic silica wafers**: Silica wafers chips were treated by ultra-sonication in a beaker filled with fresh chloroform three times for ten minutes each time. The washing with chloroform was followed by washing with alcohol using the same procedure three times. The treated silica wafers were then blown dry with high purity nitrogen followed by plasma cleaning for 20 minutes. The silica wafers treated as such were found to be extremely hydrophilic, with a water contact angle of close to 0°. These silica wafers were referred in our study as hydrophilic silica wafers.

B. Mildly hydrophobic silica wafers: Several of hydrophilic silica wafers prepared above was then baked at 1000 °C for 24 hours to eliminate the OH group on the surface with a heating rate of 10 °C/min. The heat treatment was carried out in a covered ceramic bowl to prevent dust from attaching to the wafer surface.

Silica wafers prepared in this way were found to be much more hydrophobic as indicated by a contact angle of around 43°. The hydrophobicity of silica wafers treated as such was found to be relatively stable, as rinsing with water did not reverse the contact angle back to 0°. To prevent re-hydroxlation, the baked silica wafers were sealed in a nitrogen-filled jar kept in a desiccator under room temperature until been used.

3.5.2 Experiment-silica wafer contamination test
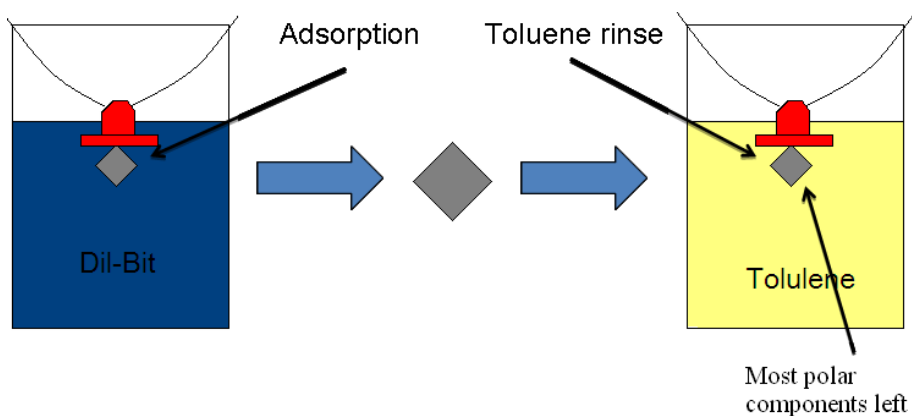
Figure 3-18. Procedure for silica wafer contamination tests.

Shown in figure 3-18, the treated silica wafers were then dipped into a 60% bitumen in either heptane or toluene solution. At this concentration, the precipitation of asphaltene will not be triggered. After been conditioned with the diluted bitumen for 4 hours, the silica wafers were taken out and rinsed extensively in a toluene-filled beaker under magnetic stirring. The rinsing time was controlled to be 15 minutes, and the rinsing procedure was repeated at least three times until the supernatant became colorless. The rinsed silica wafer was then blown dry by nitrogen flow. The wettability of these contaminated silica wafers was measured by contact angle measurement. These silica wafers were believed to have been contaminated by the most polar components of bitumen in the system, as the toluene rinsing would remove most of the hydrocarbons on the silica surface.

3.4.3 Results and discussion –silica wafer's wettability after Contamination
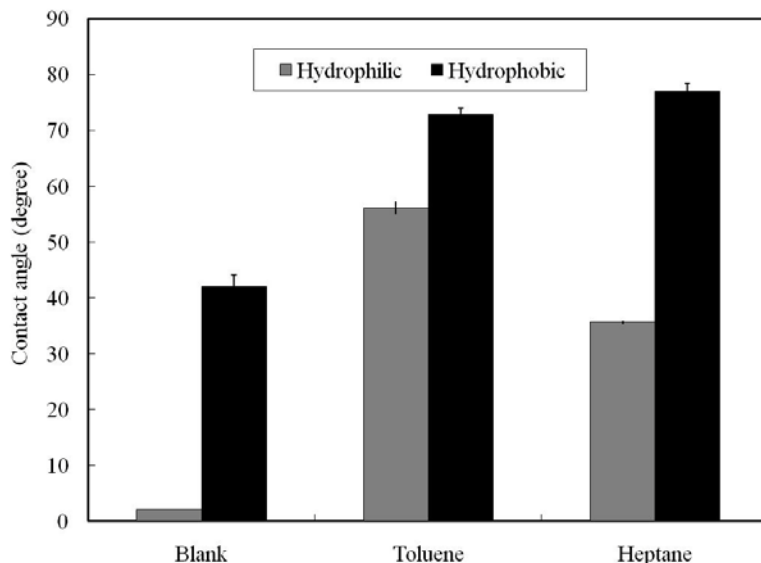
Figure 3-19. Contact angle on silica wafers before and after hydrocarbon contamination.

The x-axis of figure 3-19 shows the treatment of the silica wafers before contact angle measurement. The columns marked as "Blank" indicated the contact angle on the silica surface before contamination. Before contamination, the hydrophilic silica wafer had a contact angle of close to 0°. The baking of hydrophilic silica at 1000°C for 24 hours made it mildly hydrophobic with a contact angle of about 43°. The difference is believed to be due to the elimination of Si-OH groups on the surface, which have a stronger affinity to water molecules through the H-bonding to the oxygen atom.[64] Kondo et al. had characterized the hydroxyl groups on the surface of silica gel during the heat treatment by in situ infrared spectra.[65] They found that the intensity, position and shape of the peak for OH stretching vibration changed with heating temperature. They got a broaden peak with heating which they suppose is from the contributions of three different OH groups, the free OH groups at 3750 cm^{-1}, the weakly perturbed OH groups at 3670 cm^{-1} and the strongly hydrogen bonded OH groups at from 3300-3500 cm^{-1}. After heat treatment with temperature higher than 600°C, they found that all the strongly bonded OH groups were removed.
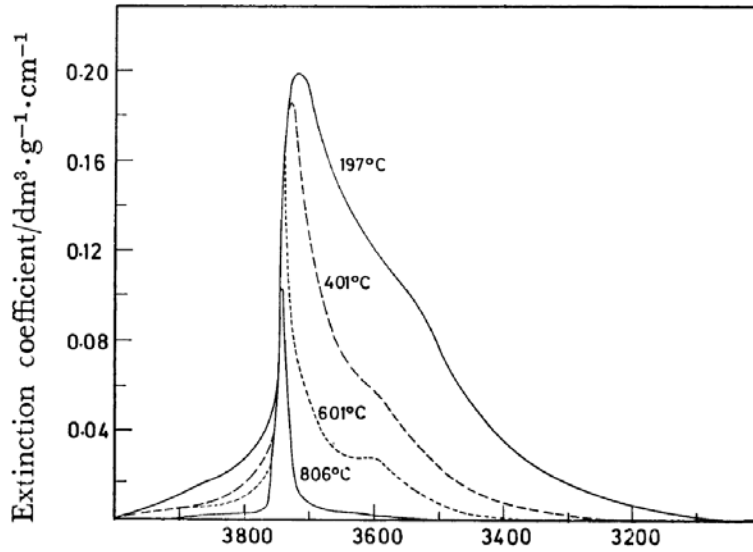
Figure 3-20. Infrared spectra of hydroxyl groups on silica with heating treatments under different temperatures.[Error! Bookmark not defined.]

The baking is believed to dehydrate the silanol (Si-OH) groups on the silica surface to form siloxan linkages (Si-O-Si).[64] The siloxan groups would be produced during the thermal treatment owing to the reaction.
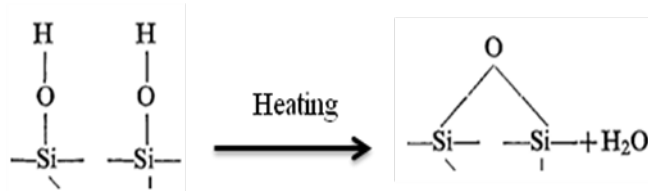
$$\text{(3–6)}$$

Compared with silanol groups, the Si-O-Si bonds are less amenable for hydrogen bonding with water molecules thereby making them less hydrophilic.

Since the silica wafers contaminated in solvent-diluted bitumen were washed with toluene extensively, the contact angles measured on the contaminated surface most likely reflect the amount of the most polar components of bitumen adsorbed onto the solids surface. It is evident that the contamination made all silica surfaces more hydrophobic as indicated by the increased contact angle. This finding reveals that toluene is not capable of washing off all the hydrocarbons

52

from the surface, even though bitumen is known to be soluble in toluene. Farid et al. proposed that these toluene insoluble organic materials (TIOM) remained on the solid surface because of their strong interactions with the host solids surface, more so when the solvent (heptane) is less favorable for dissolution of the surface-active components of bitumen.[29]

For hydrophilic silica wafers, the contact angle is significantly higher when contaminated in toluene (56°) than in heptanes (35°). This finding would indicate that the adsorption of surface-active components onto a hydrophilic surface is more favorable in a toluene-diluted environment than heptane-diluted.

It is believed that the polarity of the solvents determines the orientation of the hydrophilic functional groups of the surface-active adsorbate. In a non-polar solvent such as heptane, the hydrophilic functional groups on the hydrocarbon molecules would shield them from contacting solvents making the hydrophobic backbone facing to the solvents. Such an orientation would make the adsorption of surface-active components onto a hydrophilic surface difficult.

For the hydrophobic silica surface, however, the adsorption of surface-active components in bitumen is less sensitive to the nature of solvent. Only a slight increase in contact angle was observed for surfaces contaminated in hetpane diluted bitumen than in toluene diluted bitumen.

3.6 Washing test by different solvents

The wettability alteration is a two-way process in which the hydrocarbons in the system is adsorbed onto the solid surface when solvents are provided as an adsorption medium and the hydrocarbon molecules already adsorbed can be washed off by solvent conditioning as well. In a real case, these two effects can occur simultaneously. In this study, the de-contamination process was explored by washing the contaminated silica wafers with different solvents. Two kinds of

silica surfaces were used in this study, and the same amount of hydrocarbons was deposited on them before they were washed.

3.6.1 Sample preparation-spin coating

Figure 3-21. Spin-coater.

The spin-coater apparatus is shown in figure 3-21. The silica wafer was fastened on the chuck by applying vacuum at the bottom of the chuck. The glass hood at the top allows a small window from where the dosing syringe could insert in. When the chuck rotated at 6000 rpm, ten drops of bitumen in toluene solution with the concentration of 60% wt. were dropped onto the silica surface via a syringe. During the course of rotation, the high centrifugal force spreads the bitumen solution on the surface to form a uniform thin film on it. After two minutes, the movement of the chuck was stopped automatically by the pre-set program and the silica wafers were dried in a vacuum oven for 20 minutes at 80°C. This spin-coating process was repeated three times for each sample to ensure a complete uniform bitumen coating.

3.5.2 Experiment-washing test on contaminated silica wafer

The contaminated silica wafers prepared were then subjected to fresh solvent washing carried out in a solvents filled beaker under magnetic stirring. The washing process lasted for 15 minutes each time and was repeated until the supernatant became colorless. The washed silica wafers were then dried under nitrogen flow prior to contact angle measurements.

Beside contact angle tests using water droplets in an air environment, the tests were later also carried out using a captive air bubble method in a water environment. The purpose was to measure the contact angle change with water soaking time. Atomic Force Microscope (AFM) was used to observe the morphology of the dry surface and soaked surface.

3.5.3 Results and discussion–contact angle on surface after solvents washing
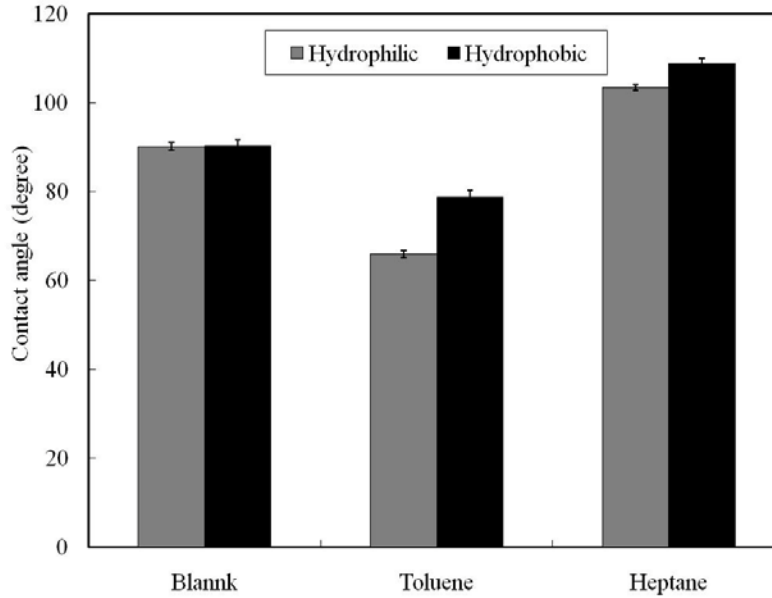
Figure 3-22. Contact angle on silica wafer before and after washing tests.

Figure 3-22 shows the contact angle on the contaminated silica surface before and after been washed with solvents. Before been washed by solvents, spin-coated bitumen surface on both hydrophilic and hydrophobic silica wafers has the same contact angle value at around 90°. This was anticipated as the bitumen was spin-coated on silica wafer surface and the wettability of silica surface beneath would have no impact on the deposition/orientation of bitumen spin-coated on solid substrate.

After toluene washing, the contact angle on the bitumen-coated silica wafers decreased, most likely due to the hydrocarbon removal from the surface. A more drastic decrease, from 90° to 65°, was found for the hydrophilic silica surface, in contrast to a decrease from 90° to 78° for hydrophobic silica wafer. This finding is consistent with the results from bitumen contamination tests in toluene, indicating that when toluene was used as solvent, the adsorption of hydrocarbons on a hydrophobic silica surface is stronger than that on a hydrophilic silica surface.

56

As opposed to the reflective surface after toluene washing, the heptane washed surface looked dull and rough due to the precipitation/aggregation of asphaltene on the surface during washing. It was interesting to note that, after heptane washing, the contact angle on the spin-coated bitumen surface increased from 90° to 105° on hydrophilic silica surface and 110° on hydrophobic silica surface respectively. This observation provided evidence that wettability is related to the type and morphology of the hydrocarbons on the surface. The increase of the contact angle was probably due to the increase of the surface roughness resulted from the precipitation of asphaltenes on the surface. The heptane wash was also anticipated to cause polar groups of asphaltene molecules to shield away from surface, exposing hydrocarbon back-bones to the surface and contributing to an increase in contact angles.

The effect of surface roughness on the wettability of solids has been studied extensively [66,67].

Figure 3-23. The effect of roughness on the observed contact angles (a). wetting drop resting on a rough surface (b). non-wetting drop resting on a rough surface. [67]

Shuttleworth et al.[68] proposed that the flow or spreading of a liquid on a rougher solid surface would be more difficult, leading to a higher contact angle. They modeled the contact angle on a rough surface θ_R as the summation of θ_0 and α_m, where θ_0 is the contact angle on the smooth surface and α_m is the slope at the contact point of liquid and solid, as schematically shown in figure 3-23.
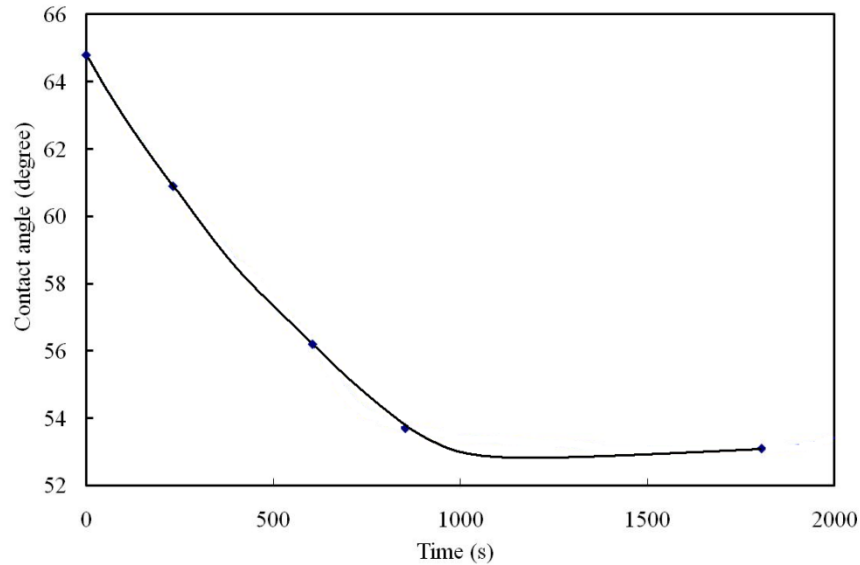
Figure 3-24. Wettability change of heptane washed silica wafer soaked in water.

The bitumen froth treatment environment is a mixed environment with solvents, bitumen, solids and water. Thus, it might also be valuable to study the wettability of asphaltene when water is present. After washing the spin coated bitumen surface by heptane, the washed surface was then immersed into a glass cell filled with water. An air bubble was then introduced onto the surface at different immersion time and the contact angle was measured. As shown in figure 3-24, the contact angle decreases with soaking time in water until a plateau of 54° was reached after 1000 seconds. It appears that after contacting with water, the hydrophilic functional groups on the asphaltenes migrated/re-oriented to the surface, which is a time dependent slow process. Such a change in molecular orientation makes the surface less hydrophobic.

To exclude the possibility that the wettability change was because of the roughness change on surface. Two asphaltene precipitated silica wafers were either dried or soaked in water for 24 hours respectively and subjected to AFM for surface imaging. It was found soaking in the water does not change the surface's roughness significantly. The roughness is 26.7nm for the dried surface and 25.4 for the soaked surface.

This finding suggests that a prolonged contact with water would change the hydrophobicity of the silica solids (the most abundant mineral in the bitumen froth) in the froth treatment, and make them more water wettable. This leads to the supposition that the water content, conditioning time and the paraffinic composition of solvents would all impact the partitioning of solids. Although it was reported earlier that the partitioning behavior of the solids could be very different when the sequence of entering the oil or water phases is different, the relationship between the water content in the system and the wettability of the solids were not reported. It would be interesting to carry out further research to understand the impact of water content on the wettability of solids.

3.6 Conclusions

- Compared with kaolinite and illite clays, siderite was found to have a higher affinity for hydrocarbon phase, and can be more easily associated with an oil droplet in a water environment.

- Siderite and kaolinite were found to be more vulnerable to hydrocarbon contamination than silica and illite.

- The increase of the paraffinic concentration in the diluent could make contaminated solids more hydrophobic, probably due to the surface precipitation of asphaltene.

- The water film on the solid surface before they were contaminated influences the contamination process for siderite and kaolinite.

- The wettability of solid surface was found to be associated with the hydrocarbons on the surface, which is influenced by the solid surface wettability and solvents environments.

CHAPTER 4 REAL FROTH SYSTEM

4.1 Introduction

In Chapter 3, the impact of solvents on the wettability of model solids was studied. It was found that solvents can change the partitioning behavior of solids between the phases. The mineral structure of the solids, their original wetting condition, and the property of solvents medium all can impact oil adsorption onto the solids surface and thus a wettability alteration.

In Chapter 4, we will study the impact of solvents on real bitumen froth solids wettability. We obtain froth samples either directly from the industrial pilot plants or extraction from the oil sands ore using a Denver Cell flotation unit. The froth samples were conditioned with different solvents and the wettability of the solids extracted from the conditioned froth was evaluated.

Three kinds of froth were used in this study. They were marked as A, B and C. Among them, froth A and B are directly from the Syncrude pilot plant and froth C was extracted from a weather low-recovery ore (ore C) by a Denver cell on the lab bench.

The film flotation technique was used to evaluate the wettability of solids extracted by centrifugation. This technique is found to be suitable for wettability evaluation on heterogeneous samples.

4.2 Materials and Methods

4.2.1 Denver cell

The setup of Denver cell flotation unit is shown in figure 4-1. The components of Denver flotation cell include a metal cell with water jacket, an air flow meter, an agitator, and a motor. If the temperature control was desired, the water jacket could be connected to a circulation bath. The agitator was connected to the motor

by a hollow rod, through which air can be supplied into the cell from an air cylinder. In a typical operation, the motor rotates to mix the water with oil sands in the cell, and air bubbles were introduced into the mixture to lift the bitumen droplets onto the top of the cell, which was then collected by a spatula. A detailed Denver Cell extraction procedure is given in Appendix II,
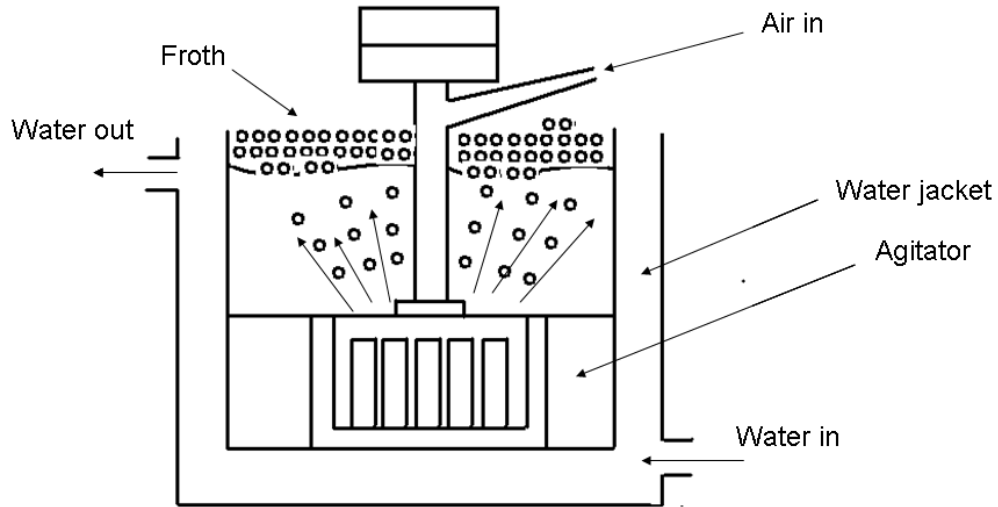
Figure 4-1. Schematic view of Denver flotation cell.

300 g of ore C were thawed under room temperature and then mixed with Syncrude process water at 35°C in the Denver cell. The mixture was conditioned at 1500 rpm for the first 5 minutes and then air bubbles were introduced into the mixture through the holes on the agitator. The airflow rate was controlled to be 180 cm^3/minute. The air bubbles would attach to the liberated oil droplets in the system and create a density difference between the attached oil and other components such as water and solids. The oil droplets captured by the air bubbles would then float to the top of the cell and form a layer of froth, which was then collected by a spatula. As the ore C is weathered, the liberation rate of bitumen is low and the bitumen froth collected was much leaner comparing with the other two kinds of froth collected from the pilot plant.

4.2.2 Dean-Stark apparatus

To measure the bitumen content of the froth C, known amount of the froth was subjected to Dean-Stark composition analysis. The Dean Stark apparatus setup is shown schematically in figure 4-2.
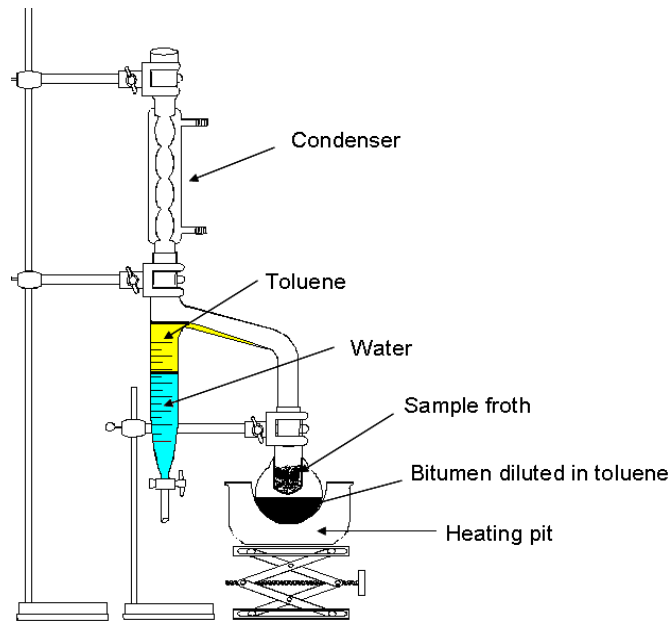
Figure 4-2. Schematic view of Dean Stark apparatus.

The Dean Stark Analysis is the most common analysis technique used in the oil sands industry to characterize the composition of products. The setup includes a heating pit, a distillation flask, a vapor condenser and a calibrated trap. A filter paper thimble is supported by the neck of the distillation flask to hold the froth samples.

250ml fresh toluene was filled into the flask and boiled by the heating pit. The toluene and water boiled would travel upwards into the condenser, and get condensed into the calibrated trap where they separated into two phases. Toluene, as the upper phase would reflux into the thimble and wash off the bitumen into the distillation flask. The operation was stopped when the solution dripping from the thimble into the flask looked colorless, indicating all the extractable bitumen was removed by toluene reflux. After the operation, the testing froth would be

separated into three phases, that are a water phase in the water trap, a cleaned solids phase in the thimble, and a bitumen solution phase in the flask. A detailed experimental procedure is given in Appendix III.

4.3 Sample preparation -solids extraction

Two kinds of solids samples were extracted from the diluted bitumen froth. They were named as combined solids sample (CSS) and partitioned solids sample (PSS). The partitioned solids sample is the sample with water-wet solids (WWS) being separated from oil-wet solids (OWS) and the combined solids sample (CSS) are the combination of them two. In the paragraphs discussed below, these acronyms are used to indicate the preparation solids received.

4.3.1 Combined solids sample (CSS) Extraction

Froth A stored in 1 L jars was heated up to 85°C in water bath followed by the addition of solvents to a solvent/bitumen weight ratio of 0.7. (The bitumen content in the industrial froth was assumed to be 60%) The mixture was conditioned on a Spex shaker for 10 minutes to loosen the bitumen at the bottom of the jar and then subjected to an impeller mixing at 1000rpm for 30 minutes. The diluted froth was then transferred into several centrifuge tubes and subjected to centrifugation at 20,000 G force for 30 minutes to remove the solids from the mixture. After the centrifugation, three phases were formed, a compact solids layer at the bottom, a supernatant diluted oil phase at the top and separated clear water layer between them. The oil phase and free water was then decanted and DI water was added to further wash off the free oil and solvents trapped in the sediment layer. The washing process was carried out on a shaker for 5 minutes. This was repeated many times until no oil could be further washed off. The washed froth solids were then transferred onto a flat weighing dish and dried in a vacuum oven at 80°C over night.

4.3.2 Partitioned solids sample (PSS) Extraction

After the dilution and impeller conditioning for another batch of froth A, 50ml of the diluted froth A was taken into a jar followed by the addition of 150ml hot DI water (80°C). The mixture was then shaken vigorously for 10 minutes before being transferred into a separation funnel where the separation of two phases were observed, a hydrocarbon phase contains diluted bitumen, emulsified water and oil-wet solids (OWS) and an aqueous phase with dispersed water-wet solids (WWS). This partitioning process was repeated four times until the amount of solids that partitioned into the aqueous phase was depleted as noted by a clear water phase after partitioning. The two phases were collected into centrifuge tubes and a centrifugation (20,000g) was applied to extract the solids in each phase. The extracted solids were washed with DI water until no oil could be further washed off and then dried in a vacuum oven. The extracted solids from the oil and water phase were labeled as OWS and WWS respectively. Labels of OWS-H and OWS-T refer to the OWS extracted from heptane and toluene diluted bitumen froth respectively. Similarly, WWS-H and WWS-T refer to the WWS extracted from heptane and toluene diluted bitumen froth respectively

4.4 Solids mineralogy characterization

4.4.1 Experiment-XRD analysis

Solids separated from the two phases were subjected to XRD characterization. Please refer to Appendix IV for detailed experimental procedure.

4.4.2 Results and discussions-XRD analysis

Samples of OWS-H, OWS-T, WWS-H, and WWS-T were sent to AGAT Laboratories Ltd. for bulk and clay XRD mineralogy composition analysis. The samples were dispersed well in DI water in an ultrasonic bath using sodium metaphosphate as a deflocculating agent. The materials were then centrifuged at

different speed in order to separates the clay and fine fraction (<3 micron) from the bulk materials (>3 micron). The weight fractions were measured for both bulk and clay portions of the samples.

Unexpectedly, it was found that the partitioning of solids is not strongly related to their size. The fraction ratio of clay/fines to bulk materials (coarser solids) is generally the same for samples extracted from the hydrocarbon and aqueous phase. This indicates that hydrophobicity is a dominant factor here in determining the solids' partitioning behavior. On a mineralogical perspective, quartz, feldspar, pyrite, and siderite were only found in bulk materials and clays such as kaolinite and illite were found in both of the size fractions.

Appendix V provides a table of mineralogical composition in each size fraction of the different solid samples. Kaolinite, illite, quarz, pyrite, feldspar and siderite were found in all of the four samples submitted but the distribution of minerals showed a significant difference between phases from where they were extracted. Figure 4-3 shows the partitioning behavior of different minerals of real bitumen froth systems.

Figure 4-3(a) shows the types of solids in the hydrocarbon phase and figure 4-3(b) shows the type of solids in the aqueous phase. The grey and black columns represent the toluene-diluted system and heptane-diluted system respectively.
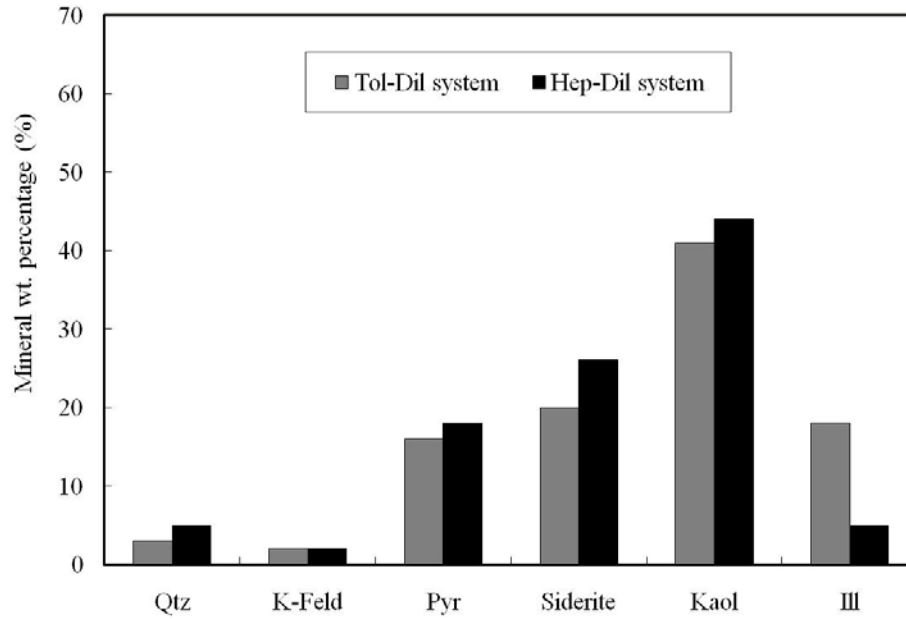
(a)
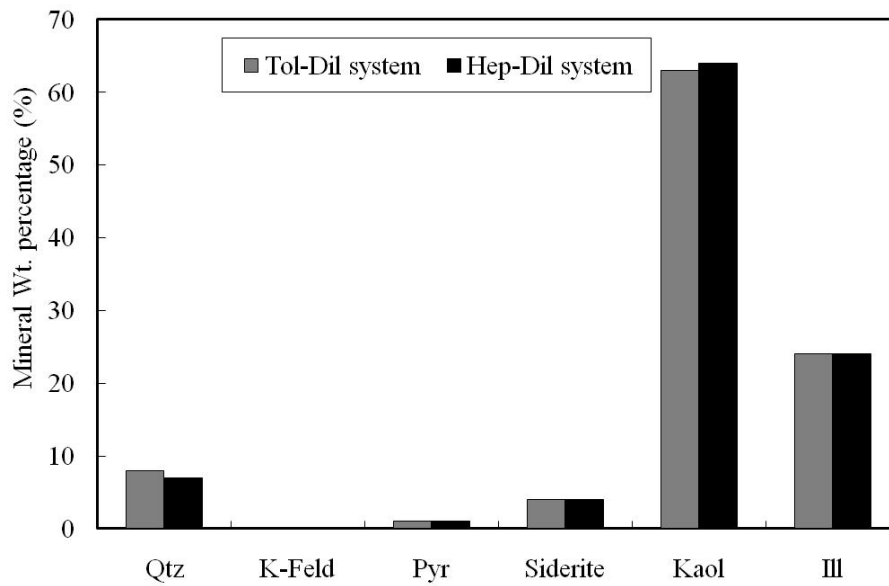
(b)

Figure 4-3. Mineralogy distribution in different phases.
(a) Solids mineralogy distribution in hydrocarbon phase .(b) Solids
mineralogy distribution in aqueous phase.

By comparing figure 4-3(a) with figure 4-3(b), it was found that different minerals have different preferences to partition into different phases. More kaolinite, illite, and quarz percentages were found in the aqueous phase, and significantly more feldspar, pyrite and siderite minerals were found in the hydrocarbon phase. The

siderite result corresponds very well with the model mineral contamination and partitioning tests described in Chapter 3, where siderite were found to be more vulnerable to hydrocarbon contamination and have higher tendency than other minerals to accumulate into the hydrocarbon layer. The partitioning difference due to different solvents is less significant here, but still noticeable. More quartz, pyrite, siderite and kaolinite were found in the hydrocarbon phase of the heptane-diluted bitumen. The preferential partitioning of kaolinite, quartz and siderite to heptane-diluted bitumen phase may be explained by the results from the model system that solids after contamination became more hydrophobic when heptane was used as solvent. For illite, the oil phase partitioning selectivity was shown towards the toluene diluted system.

4.5 Wettability evaluation- film flotation tests

The extracted solids from the froth, after being dried, were subjected to wettability evaluation analysis. Instead of using CA measurement and WDPT tests, we used another wettability evaluation technique called film flotation test. The CA measurement and WDPT were expected to be less efficient in this case due to heterogeneous nature of the natural froth solids. Film flotation test was proved effective with particles that display mixed levels of wettability.

The film flotation technique was first developed by researchers in the University of California Berkeley to characterize the wetting behaviors of coal particles[47, 48]. The advantage of this technique is that it enables the determination of the particles critical wetting surface tension, which is the largest surface tension the liquid could have, to completely wet the particles surface. In the film flotation test, the testing particles were carefully sprinkled onto the surface of probing liquid, and they would only sink through the liquid/air interface when the surface tension of the liquid is equal or smaller to its critical wetting surface tension, and this phenomenon is majorly governed by the surface energy properties between the solids and liquid. The effect of solids size and density are negligible within a very wide range.

By altering the surface tension of the liquid, the accumulative weight percentage of sinking solids could be plotted with the changing surface tension to obtain the minimum and maximum critical wetting surface tension of the testing particles. Another important feature of this technique is that it can deal with samples that are heterogeneous in wettability, and give detailed information on the weight percentage of solids in a certain wettability range. Thus, the film flotation technique was chosen in this study to measure the froth solids samples.

4.5.2 Experiment
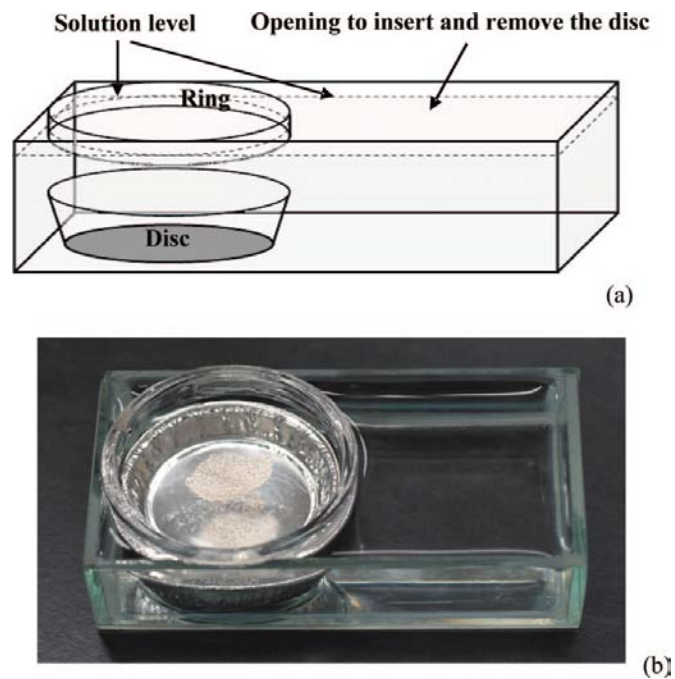
Figure 4-4. Film flotation apparatus.
a. Film flotation apparatus setup. b. Solids sprinkled on the surface of solution.[53]

The apparatus shown in figure 4-4 was designed and manufactured. A glass ring with the diameter of 50 mm was attached to a 120mm × 50mm × 20mm open glass dish. The height of the ring was approximately 10 mm, giving enough space for a 40mm × 4mm foil weighing-dish to be inserted to the bottom. Nine different methanol/water solutions were prepared with the volume concentration ranging from 10% to 90%. The surface tension of these solutions and that of the pure

methanol and DI water was measured by a KRÜSS processor tensiometer (model K100MK2). The weighing dishes in this experiment were carefully weighed before use. During the measurements, the glass dish was filled with methanol/water solution. The dried solids sediment obtained in Section 4.2 were crushed by a motar-pestal set and sieved through a sieve (150µm-220 µm). Since most of the solids 'particles' within this size range are agglomerates of fine particles, it could represent the accumulative wettability of froth solids. A weight of 0.02g of each kind of solids were carefully weighed and gently sprinkled onto the surface of the solution within area of the ring to form a solids monolayer on the surface. The solids particles that sank through the interface were considered wettable by the probing liquid with the specific surface tension, and those floated on the surface were considered hydrophobic at the probing surface tension. The higher the solution surface tension, the easier for the solids to stay floating. After allowing 5 minutes for the system to reach equilibrium, the weighing dishes with wetted solids were taken out and dried in a vacuum oven at 50°C for 6 hours. The percentage of floating solids was then calculated by mass balance and plotted against the surface tension of the solutions.

4.5.3 Results and discussion

4.5.3.1 Surface tension of methanol solutions
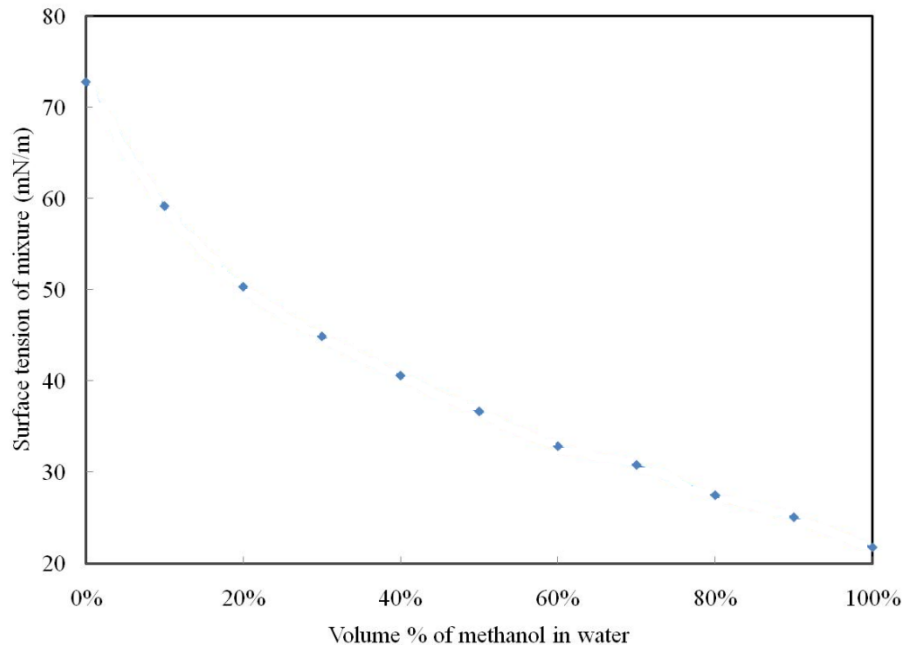
Figure 4-5. Change of surface tension with methanol volume fraction in water solutions.

The surface tension of the methanol in water solution was manipulated by changing the volume percentage of methanol in water. The relationship between surface tension of the mixture and methanol volume fraction is shown in

figure 4-5. With the increase of the methanol volume fraction, the surface tension of the mixture changed over a very wide range, which decreased from 73mN/m (the surface tension of DI water) to 21mN/m, (the surface tension of pure methanol). The relationship between the surface tension and methanol volume fractions follows a non-linear manner, which indicates that the mixing of these two components was not ideal in this case as methanol molecules have a greater tendency to accumulate at the air/ liquid interface.

4.5.3.2 Wettability of extracted oil wettable solids (OWS)
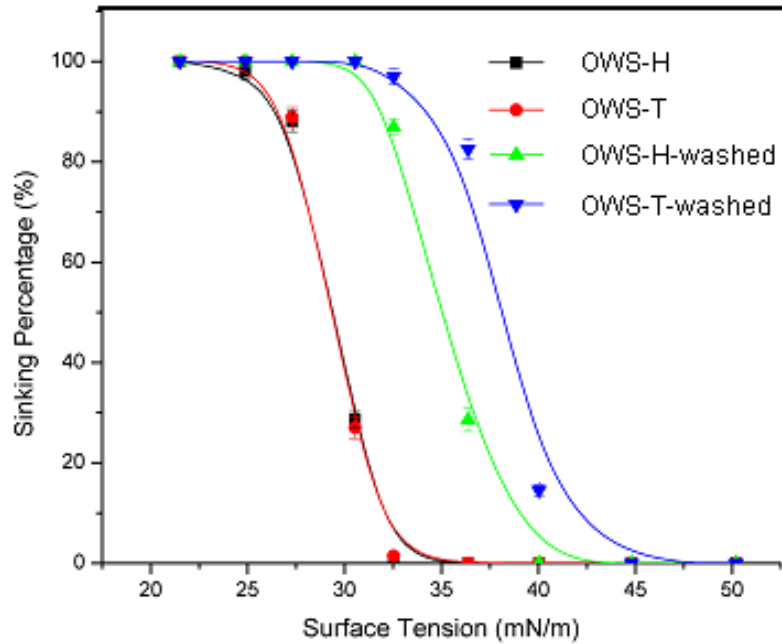
Figure 4-6. Accumulative film flotation curves of OWS from froth A before and after been washed by fresh solvents.

Figure 4-6 shows the film flotation curve of OWS from the heptane-diluted system (black curve) and toluene-diluted system (red curve). The solids were named as OWS-H and OWS-T respectively. It was found that the film flotation curves of OWS-H and OWS-T solids fell at the same location within a narrow critical wetting surface tension range from 26mN/m to 37mN/m. This indicated that these two kinds of solids have very similar level of hydrophobicity. The similarity in wettability might be resulted from the overly covered surface of OWS-H and OWS-T by bitumen. As there was no exposed clean solids surface, the wettability was only determined by the bitumen and not influenced by the solid surface.

The solids extracted from the hydrocarbon phase were then extensively washed by heptane or toluene until the supernatant became colorless, and then dried. It was observed that after washing, the film flotation curves shifted to the right hand side, indicating a more hydrophilic nature after washing. The toluene washed

solids is more hydrophilic than heptane washed solids, which was anticipated as the heptane solvent does not dissolve asphaltene from the surface.
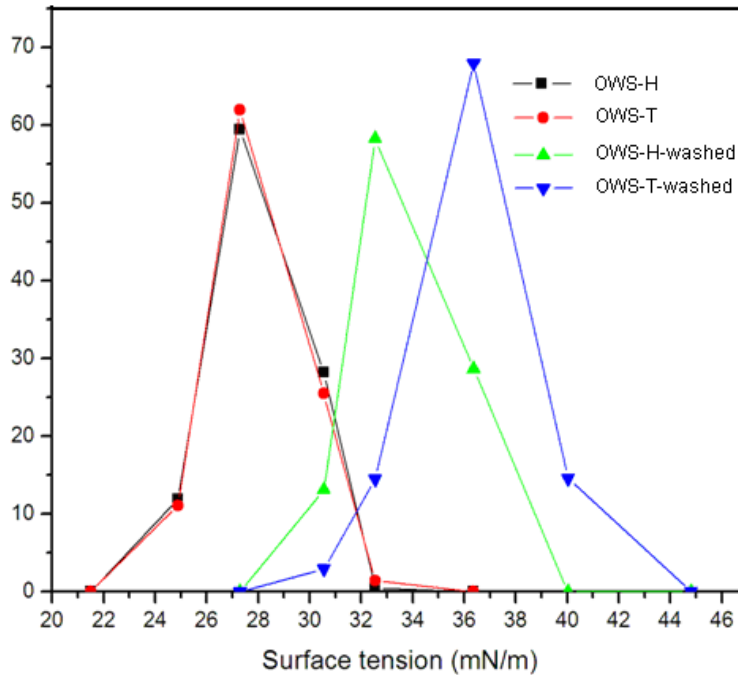
Figure 4-7. Frequency of the film flotation curve of OWS before and after been washed by fresh solvents.

Frequency distribution of the film flotation curves of hydrophobic solids is shown in figure 4-7. The frequency distribution curves reveal the percentage of solids in each critical wetting surface tension range. Before extensive solvent washing, the critical wetting surface tension for OWS-H and OWS-T fell into the range from 21mn/m to 33mN/m. After heptane or toluene washing, their critical wetting surface tension fell into the range of 27mN/m-40mN/m and 31mN/m-45mN/m, respectively. Based on the supposition that the un-washed surface of OWS solids are almost overly covered by bitumen, heptane washed OWS surface are partially covered by bitumen and toluene washed OWS are nearly free of bitumen, these results suggested that the bitumen surface and original OWS solid surface have a critical wetting surface tension range of 21-33 mN/m and 31-45mN/m, respectively. The surface that was partially covered by bitumen has a critical wetting surface tension within the range of 27-40mN/m.

4.5.3.2 Wettability of extracted water wettable solids (WWS)
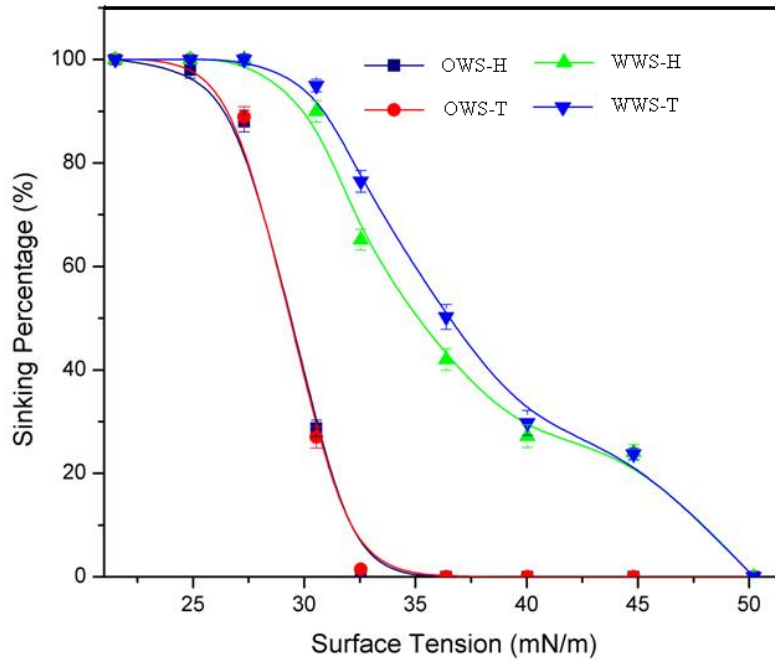
Figure 4-8. Accumulative film flotation curves for WWS and OWS.

The solids extracted from the aqueous phase are referred as WWS. Their film flotation curves were plotted together with the curve for OWS in figure 4-8 to make a comparison. It was found that the WWS were much more hydrophilic than OWS, as indicated by curve shifting to the right. A significant portion of the solids fell into the surface tension range from 35mN/m-50mN/m. There is a slight hydrophobicity difference between the hydrophilic solids from different solvent systems. The WWS-T is slightly more hydrophilic than WWS-H.
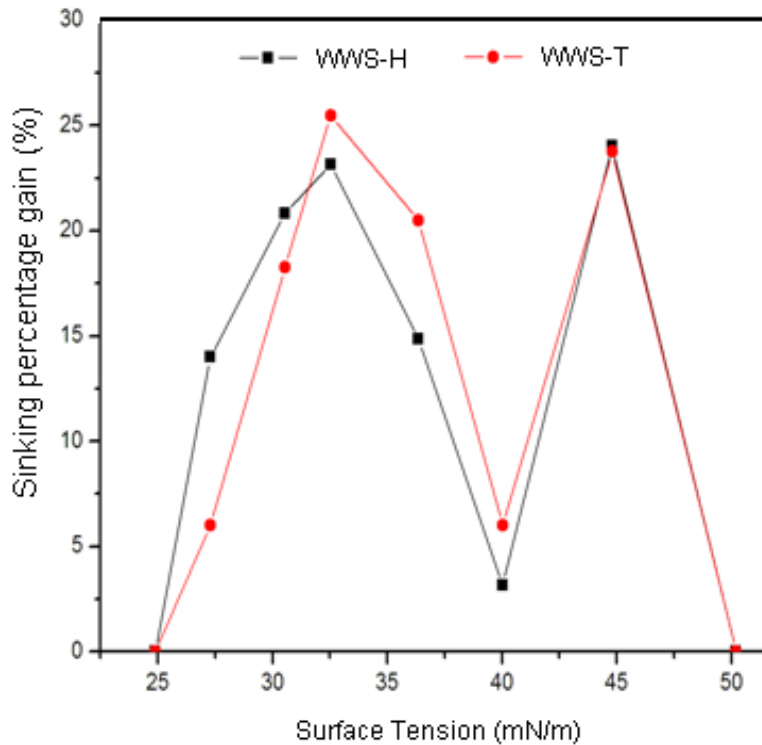
Figure 4-9. Frequency of the film flotation curve for WWS.

Figure 4-9 shows the frequency of the wettability curves for WWS-H and WWS-T. It was very interesting to note that the curve was bimodal for both of the systems. This indicated that there were two hydrophobicity levels in the WWS. The first peak ranges from 25mN/m-40mN/m. This range corresponds very well with the peak of OWS after heptane-washing. As the heptane would leave the asphaltene components of the bitumen behind, this critical wetting surface tension range could represent the solids that were partially covered by hydrocarbons. This suggests that the solid surface partially covered by bitumen, with the critical surface tension falls into the range of 28mN/m-32mN/m (the overlapped region of the critical surface tension range of hydrophobic and hydrophilic solids) would have chance to partition into either the hydrocarbon phase or aqueous phase. The solids with a critical surface tension larger than 32mN/m could end up in the aqueous phase after partitioning tests. Another peak in the histogram ranges from 40mN/m-50mN/m. This is a very hydrophilic region, as this region is not found in the wettability curves of washed OWS-T, which were washed by toluene extensively to have most of its surface-hydrocarbons removed. It is supposed that

75

the critical surface tension region from 40mN/m-50mN/m stands for the wettability of the most hydrophilic minerals in the system. This fraction of the minerals might be of not contaminated by hydrocarbons at all.

4.5.3.3 Wettability of combined solids samples (CSS)
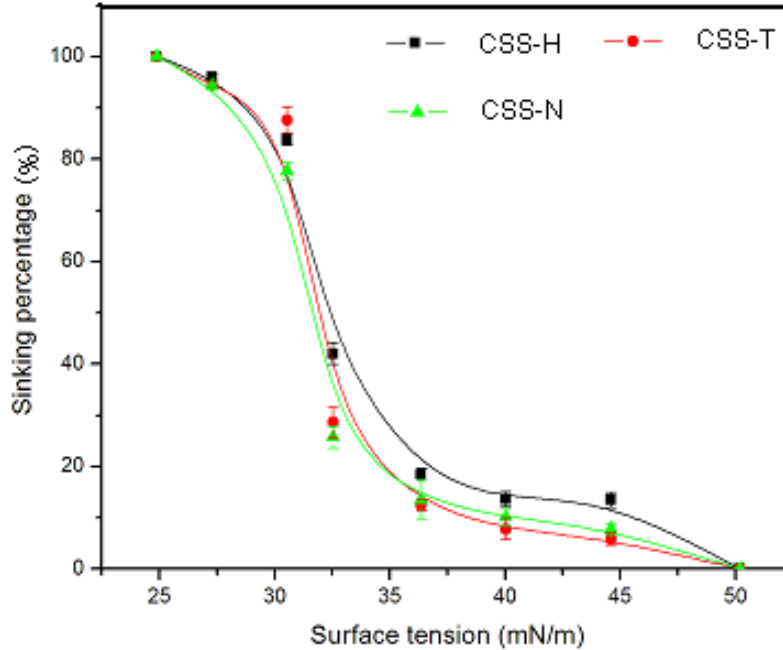
Figure 4-10. Accumulative film flotation curves for CSS extracted by different solvents.

Figure 4-10 shows the film flotation curved for the CSS which were extracted from the froth A that was diluted by either heptane, toluene or naphtha. The solids samples were referred as CSS-H, CSS-T and CSS-N (CSS-N refers to CSS extracted from naphtha diluted bitumen froth), respectively. According to the positions of the curves, the wettability of CSS-T and CSS-N are very similar while the CSS-H has a more hydrophilic nature on average. However, generally, the critical wetting surface tension of them all fell into the range from 25mN/m-50mN/m.
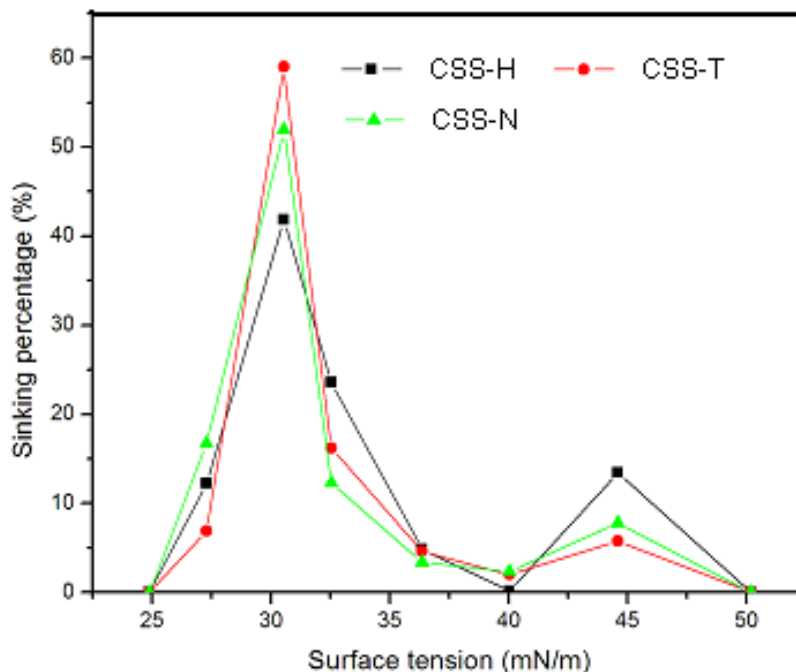
Figure 4-11. Frequency of film flotation curves for CSS extracted by different solvents.

The frequency of the "combined solids" film flotation curves based on the average sinking percentage at different surface tensions are shown in figure 4-11. All of them are bimodal curves with two regions from 25mN/m-40mN/m and 40mn/m-50mN/m. The differences in solids wettability for these three systems are more obvious here when plotted as histograms. A 15wt% of the solids fell into the hydrophilic region (critical surface tension range from 40mN/m to 50mN/m) in the heptane diluted system, while this value is 8wt% and 5wt% for the toluene and naphtha diluted system respectively. It would be complicated to compare wettability of CSS in the hydrophobic region (25mN/m-40mN/m) as the curves intersected with each other in this region. Here, it may be instructive to separate the hydrophobic region further into three sub-regions, namely a less hydrophobic region (32.5mN/m-40mN/m), a medium hydrophobic region (30mn/m-32.5mN/m) and a highly hydrophobic region (25mn/m-32.5mN/m). The sinking percentage comparisons are:

In the less hydrophobic region, CSS-H>CSS-T> CSS-N.

In the medium hydrophobic region, CSS-T> CSS- N> CSS- H.

In the highly hydrophobic region, CSS- N> CSS- T> CSS- H.

The broadness of the peak reveals the heterogeneity of the solids wettability. It is found that the solids extracted from the heptane-diluted system have the most heterogeneous wettability and the solids from the toluene-diluted have the most homogenous wettability. A trend was shown that with the increase of paraffinic content in the solvents, the heterogeneity in solids wettability increases as well.

4.6 The impact of ore sources on the solids wettability

One of the challenges in oil sands research is that the results are always heavily influenced by the ore property. Here, it is desirable to study the impact of ore on the wettability of froth solids after solvents treatment. As mentioned earlier, three kinds of froth were used in this study. Two of them were directly from the industry pilot plant, and were named as A and B. The last one was named as C, which is from a weathered ore source. CSS solids were extracted from the solvents conditioned froth and their wettability after solvents treatments was evaluated using film flotation technique.

4.6.1 Sample preparation and experiment

A and B bitumen froth samples were obtained from the extraction pilot plant at Syncrude Research Centre and were sealed in 4L metal pails for future use. Before each experiment, the bitumen froth was heated in an oven to 80°C to reduce its viscosity. The hot froth was mixed well with a large spatula before been sub-sampled into a 1L jar, where it was mixed with solvents at a solvents/bitumen weight ratio of 0.7 by weight. (While froth A and B are assumed to have a bitumen content of roughly 60%, the C froth generated by Denver flotation cell is much leaner. The Dean-Stark analysis revealed the bitumen content in froth C to be 13.3wt%)

After conditioning with solvents for 30 minutes, the solids in the diluted froth were extracted using centrifugation at a 20,000g force. The solids were washed by

water extensively following the procedure described before and were dried in a vacuum oven prior wettability evaluation.

Only CSS solids were extracted here and the wettability evaluation was based on the histogram of the accumulative wetting curves of the solids extracted.

4.6.2 Results and discussion
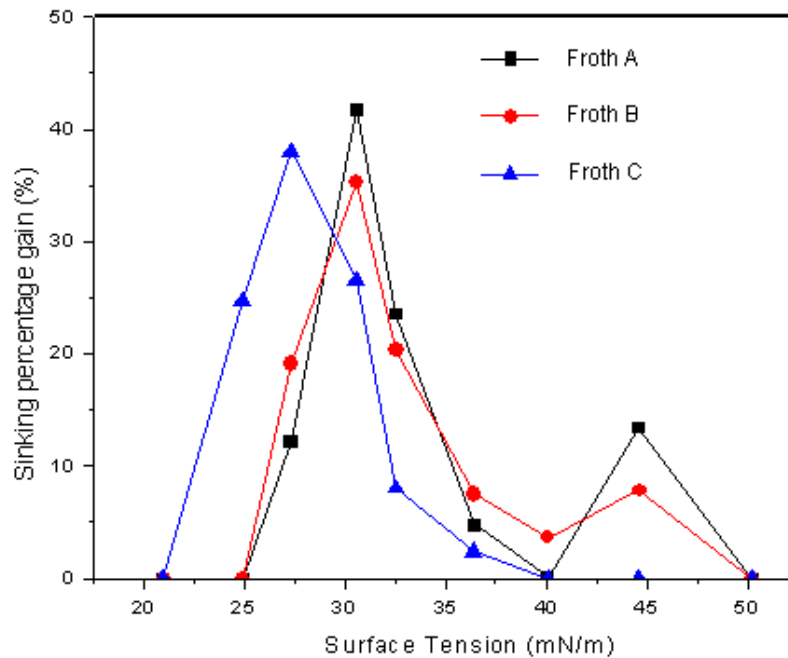
Figure 4-12. Frequency of the film flotation curve for CSS solids extracted from heptanes.

Figure 4-12 shows the histogram of the film flotation curve of CSS extracted from froth diluted by heptane. It was found that, for the solids from bitumen froth A and B, the curves are bimodal, while only one peak was found in the curve for froth C solids. The missing peak for froth C solids is the one located in the range of 40mN/m-50mN/m. This suggests that the solids from froth C have a more hydrophobic nature and 0% of them would sink at such a high surface tension range. Both froth A and B solids showed some extent of sinking behavior at the surface tension range of 40mN/m-50mN/m, indicating that in both of these samples, there were hydrophilic solids present. Comparing with froth B solids,

79

froth A solids were found to have more solids sank in this region (15% vs. 10% by weight). In the hydrophobic region, more B solids were found to be in the highly hydrophobic region while more A solids were found to be in the medium hydrophobic region. For the froth C solids, however, there are 30% of solids were found having critical surface tension smaller than 25mN/m, which indicated again that the froth C solids have a more hydrophobic nature than solids from the industrial froth.
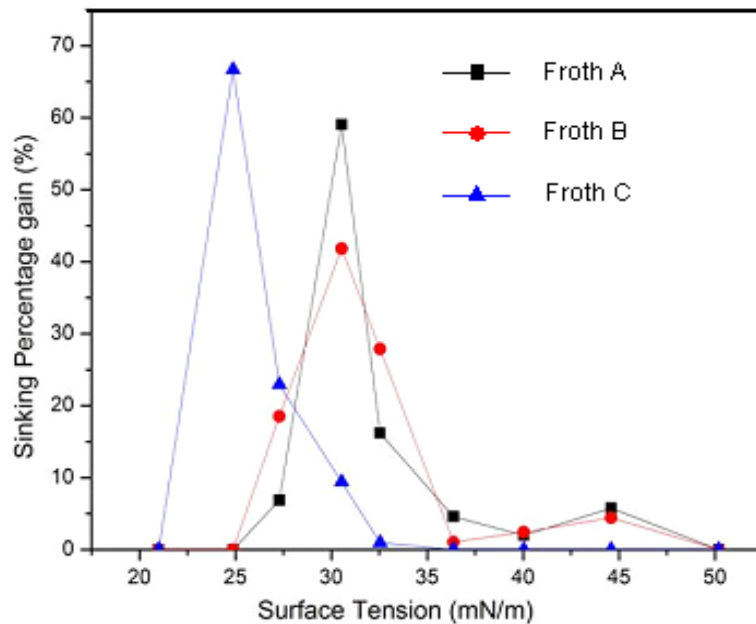
Figure 4-13. Frequency of the film flotation curves for CSS extracted from toluene.

Figure 4-13 shows the frequency of CSS from the toluene-diluted system. It shares the trends found in the heptane-diluted except the peaks found in the histogram for the toluene-diluted system are narrower than those in the heptane-diluted system. This indicates again that more wettability heterogeneity would be found in a paraffinic dominated solvent.

The results confirmed Ren et al.'s findings [69] that the weathering would force more hydrocarbon molecules onto the solid surface and make them more hydrophobic. He attributed the mechanism to the loss of water on the solid surface during weathering process.
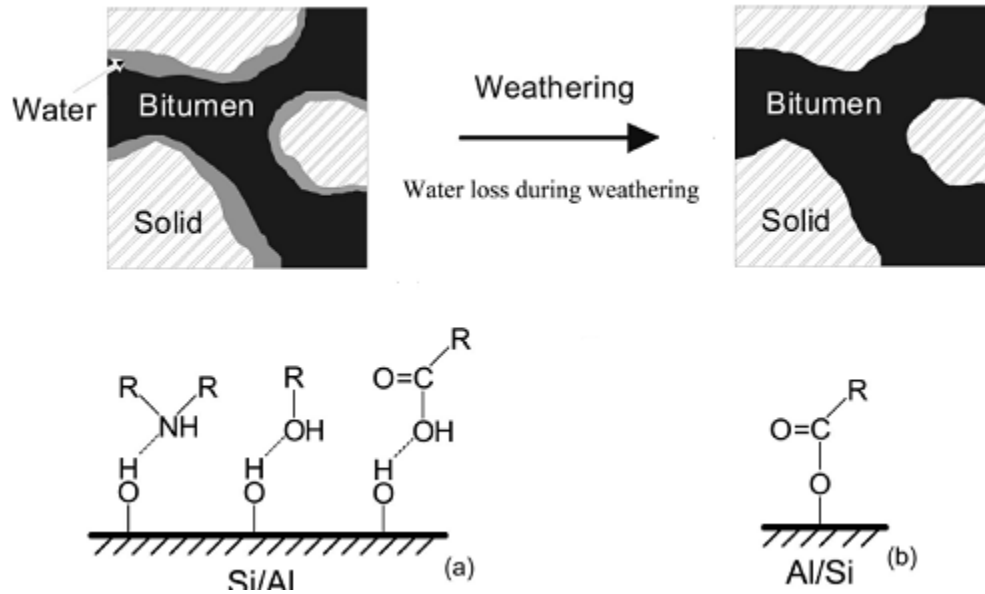
Figure 4-14 Possilbe bonds between the organic molecules and solid surface proposed by Ren. (a). Hydrogen bonds. (b). chemical bonds. [69]

He proposed the mechanism as shown in figure 4-14 that with the elimination of water film, hydrocarbon molecules would easily strongly adsorbed onto the surface through either hydrogen bonds or chemical bonds.

4.7 Conclusions

- The hydrocarbon and aqueous phases after froth partitioning were found to have different mineral distributions. Siderite and pyrite were found to have higher tendency to stay in the hydrocarbon phase while kaolinite, quarz, silica and illite more readily report to the aqueous phase.

- Film Flotation was found to be a good wettability evaluation technique for bitumen froth solids that have higher wettability heterogeneity.

- Higher wettability heterogeneity was found in solids extracted from a heptane diluted system for all of the three froth samples studied.

- The solids partitioning between phases is directly related to the solids wettability which is heavily determined by the hydrocarbons on the surface.

- Solids reporting to the water phase were found having two different levels of hydrophobicity, as indicated by their critical wetting surface tension.

- Wettability is also related to the ore source. The froth solids from weathered ore used in this study were found to be much more hydrophobic and having a critical wetting surface tension lower than 40mN/m.

CHAPTER 5 SUMMARY AND FUTURE WORK

Using model minerals and real bitumen froth minerals, in this work we studied solids wettability alteration by changing solvents composition in a bitumen froth treatment environment.

In the model systems, the solids vulnerability to hydrocarbon contamination was found to be different on the mineralogical perspective, and the solvents composition was found to be associated with mineral partitioning and solids surface hydrocarbon content change. The XRD analysis on the solids type in different phase in a real froth system confirmed the partitioning behavior difference observed in model solids system, however, the wettability change of real froth solids with solvents type is not as significant as observed in model system.

The future work could be more focused on establishing the naphtha type impact on the solid wettability change. It would be desirable to study the hydrocarbon composition after different solvents washing, and establish a relationship between the wettability, hydrocarbon composition remained on the solid surface and solvents property.

REFERENCES

1. J. Masliyah, Z. Zhou, Z. Xu, "Understanding water-based bitumen extraction from Athabasca oil sands", *The Canadian journal of chemical engineering,* 82(4), 628-654 (2004)

2. ST 98-2009: Alberta's energy reserves 208 and supply/demand outlook 2009-2018

3. J. Masliyah, "Fundamentals of oil sands extraction", course materials at University of Alberta

4. E. C. Sanford, F. A. Seyer, "Processability of Athabasca tar sand using a batch extraction unit: the role of NaOH", *CIM bulletin*, 3, 164–169 (1979)

5. U. G. Romanova, H. Yarranton, L. L. Schramm, "Investigation of oil sands froth treatment", *The Canadian journal of chemical engineering,* 82(4), 710-721 (2004)

6. Y. C. Long, T. Dabros, H. Hamaz, "Stability and settling characteristics of solvent-diluted bitumen emulsions", *Fuel*, 81(15), 1945-1952 (2002)

7. P. Bayliss, A. A. Levinson, "Mineralogical review of the Alberta oil sand deposits (Lower Cretaceous, Mannville Group)", *Bulletin of Canadian Petroleum Geology,* 24, 211–214 (1976)

8. F. W. Camp, "Processing Athabasca tar sands—tailings disposal", *Proceedings of the 26th Canadian Chemical Engineering Conference* (1976a)

9. J. A. Ripmeester, L. S. Kotlyar, B. D. Sparks, "Structure and properties of oil sands and clay tailings of colloidal clays," *Colloids and Surfaces*, A (78), 57–63 (1993)

10. M. A. Kessick,"Structure and properties of oil sands and clay tailings", *Journal of Canadian Petroleum Technology*, 18(1), 49–52 (1979)

11. R. N. Yong, and A. J. Sethi, "Mineral particle interaction control of tar sand sludge stability," *Journal of Canadian Petroleum Technology*, 77(4), 76–83 (1978)

12. H. Kaminsky, T. H. Etsell, D. Ivey "Distribution of clay minerals in the process streams produced by the extraction of bitumen from Athabasca oil sands", *The Canadian Journal of Chemical Engineering,* 87(1), 85-93 (2009)

13. R. Tipman, Y. C. Long, "Solvent process for bitumen separation from oil sands froth ", *US patent 5876592*

14. L. Kotlyar, B. Sparks, J. Woods, "Distribution and types of solids associated with bitumen", *Petroleum Science and Technology,* 16(1-2), 1-19 (1998)

15. F. Bensebaa, L. Kotlyar, B. Sparks, "Organic coated solids in Athabasca bitumen characterization and process implications", *The Canadian Journal of Chemical Engineering,* 78(4), 610-616 (2000)

16. K. Darcovich, L. Kotlyar, W.Tsem, "Wettability study of organic rich solids separated from Athabasca oil sands", *Energy & Fuels,* 3(3), 386-391 (1989)

17. Y. Yan and J. H. Masliyah,"Solids-stabilized oil in water emulsions: scavenging of emulsion droplets by fresh oil addition" *Colloids and Surfaces. A* ,75, 123 (1993)

18. X. Yang, W.Tan, Y. Bu, "Demulsification of asphaltenes and resins stabilized emulsions via the freeze/thaw method", *Energy & Fuels, 23(1),* 481-486 (2009)

19. J. Stark , S. Asomaning, "Synergies between asphaltene stabilizers and demulsifying agents giving improved demulsification of asphaltene-stabilized emulsions", *Energy &Fuels,* 19(4), 1342-1345 (2005)

20. L. Xia, S. Lu, G. Cao, "Stability and demulsification of emulsions stabilized by asphaltenes or resins", *Journal of Colloid and Interface Science,* 271(2), 504-506 (2004)

21. A. Yeung, T. Dabros and J. Masliyah, "On the interfacial properties of micrometre-sized water droplets in crude oil", *proceedings - Royal Society. Mathematical, physical and engineering sciences,* 455(1990), 3709-3723 (1999)

22. A. Yeung, T. Dabros and J. Masliyah, "Micropipette: a new technique in emulsion research", *Colloids and Surfaces. A, Physicochemical and engineering aspects,* 174(1-2), 169-181 (2000)

23. J. D. McLean, P. K. Kilpatrick, "Effects of asphaltene solvency on stability of water-in-crude-oil emulsions", *Journal of Colloid and Interface Science,* 189 (2), 242-253 (1997)

24. Z. Yan, J. Elliott, J. Masliyah, "Roles of various bitumen components in the stability of water-in-diluted-bitumen emulsions", *Journal of Colloid and Interface Science*, 220(2), 329-337 (1999)

25. J. Strassner, "Effect of pH on interfacial films and stability of crude oil water emulsions", *Journal of Petroleum Technology*, *20(3)*, 303 (1968)

26. M. Ese, K. Gawrys, P. Spiecker, "Asphaltene and naphthenate mechanisms of emulsion stabilization in water-in-crude oil emulsions", *Abstracts of papers of the America chemical society,* 23, U678-U678 (2003)

27. P. Spiecker, A. Sullivan, N. Zaki, "Use of interfacial film rheology and critical electric field measurements to relate asphaltene film properties to crude and model oil emulsion stability", *Abstracts of papers of the America chemical society,* 219, U703-U703 (2000)

28. A. Sullivan, N. Zaki, J. Sjoblom, "The stability of water-in-crude and model oil emulsions", *The Canadian Journal of Chemical Engineering,* 85(6), 793-807 (2007)

29. F. Bensebaa, L. Kotlyar, B. Sparks and K. Chung, "Organic coated solids in Athabasca bitumen: characterization and process implications", *The Canadian Journal of Chemical Engineering,* 78 (August), 610–616 (2000)

30. D. Sztukowski , H. Yarranton ,"Characterization and interfacial behavior of oil sands solids implicated in emulsion stability", *Journal of Dispersion Science and Technology*, 25(3), 299–310 (2004)

31. D. Saukowski and H. Yarranton, "Oilfield solids and water-in-oil emulsion stability", *Journal of colloid and interface science,* 285(2), 821-833 (2005)

32. M. Poindexter, S. Chuai and R. Marble, "Solid Content Dominates Emulsion Stability Predictions"**,** *Energy & Fuels, 19(4),* 1346-1352 (2005)

33. A. Wu, "Selective creaming: A novel technique to isolate interfacial organics and mineral solids from water-in-oil emulsions", *Energy & fuels,* 22(4), 2346-2352 (2008)

34. J. Liu, Z. Xu, J. Masliyah, "Processability of oil sand ores in Alberta", *Energy Fuels,* 19(5), 2056–2063 (2005)

35. N. Yan, Y. Maham, J. Masliyah, M.Gray, A. Mather, "Measurement of contact angles for fumed silica nanospheres using heat of immersion data", *Colloids and Interface Science,* 228(1), 1–6 (2000)

36. S. Levine, B. Bowen, S. Partridge, "Stabilization of emulsions by fine particles I. Partitioning of particles between continuous phase and oil/water interface", *Colloids and Surfaces*, 38(4), 325–343 (1989)

37. M. Hoeben, R.Van der Lans, L.Van der Wielen, "Kinetic model for separation of particle mixtures by interfacial partitioning", *AIChE Journal*, 50(6), 1156–1168 (2005)

38. B. Binks, S. Lumsdon, "Effects of oil type and aqueous phase composition on oil–water mixtures containing particles of intermediate hydrophobicity", *Physical Chemistry Chemical Physics,* 2(13), 2959–2967 (2000)

39. F. Chen, J. Finch, Z. Xu, J. Czarnecki, "Wettability of fine solids extracted from bitumen froth", *Journal of Adhesion Science and Technology*, 13(10), 1209–1224 (1999)

40. Y. He, J. Laskowski, "Contact angle measurements on discs compressed from fine coal*", Coal Preparation,* 10, 19–36 (1992)

41. N. Yan, M. Gray, J. Masliyah, "On water-in-oil emulsions stabilized by fine solids", *Colloids and Surfaces A: Physicochemical and Engineering Aspects,* 193(1-3), 97–107 (2001)

42. A. Hannisdal, M. Ese, P. Hemmingsen, J. Sjoblom, "Particle-stabilized emulsions:effect of heavy crude oil components pre-adsorbed onto stabilizing solids", *Colloids and Surfaces A: Physicochemical and Engineering Aspects* 276(1-3), 45–58 (2006)

43. P. Herrtjes, N. Kossen, "Measuring the contact angles of powder-liquid systems", *Powder Technology*, 1, 33–42 (1967)

44. N. Kossen, P. Heertjes, "The determination of the contact angle for system with a powder", *Chemical Engineering Science*, 20, 593–599 (1965)

45. C. Jouany, P. Chassin, "Determination of the surface energy of clay-organic complexes by contact angle measurements", *Colloids and Surfaces,* 27(4), 289–303 (1987)

46. E. W. Washburn, "The Dynamics of capillary flow*" Physical Review*, 17(3), 273 - 283 (1921)

47. D. Fuerstenau, J. Diao, M. Williams, "Characterization of the wettability of solids particles by film flotation 1. experimental Investigation" *Colloids and Surfaces*, 60, 127-144 (1991)

48. J. Diao, D. Fuerstenau "Characterization of the wettability of solid particles by filmfloation.2.theoretical analysis. "*Colloids and surfaces,* 60, 145-160 (1991)

49. J. Sablik, K.Wierzchowski, "Evalution of the Influence of flotation reagents on the hydrophobicity of coal using the film flotation method" , *Fuel,* 71(4), 474-475 (1992)

50. R. Matherm D.Taylor "Investigation of the heterogeneity of organic pigment particle surfaces using a film flotation method", *Dyes and pigments,* 43(1), 47-50 (1999)

51. B. S. Furnell et al., "*Vogel's Textbook of Practical Organic Chemistry*", 5th edition, Longman/Wiley, New York, (1989)

53. T. Dang-Vu, R. Jha, S. Wu, "Wettability determination of solids isolated from oil sands", *Colloids and surfaces. A, Physicochemical and Engineering Aspects,* 337(1-3), 80-90 (2009)

54. R. Xu, "Particle Characterization: Light Scattering Methods", Kluwer Academic Publishers, Dordrecht (2000)

55. R, Al-Maamari, J. Buckley "Asphaltene precipitation and alteration of wetting: The potential for wettability changes during oil production", *SPE Reservoir Evaluation & Engineering,* 6(4), 210-214 (2003)

56. J. Buckley, "Wetting alteration of solid surfaces by crude oils and their asphaltenes", *Revue de l'Institut français du pétrole,* 53(3), 303-312 (1998)

57. Y. Liu, J. Buckley "Evolution of wetting alteration by adsorption from crude oil", *SPE Formation Evaluation,* 12(1), 5-11 (1997)

58. J. Buckley, "Predicting the onset of asphaltene precipitation from refractive index measurements", *Energy & Fuels*, 13(2), 328-332 (1999)

59. W.A.Deer, R.A. Howie, and J. Zussman, "An introduction to the rock-forming minerals (2nd ed.)", Harlow: Longman, (1992)

60. A .Meunier, B.Velde, " Illite: origins, evolution, and metamorphism", Springer-Verlag Berlin Geidelberg (2004)

61. J. L. Bantignies, C.C.D.Moulin, H.Dexpert "Wettability contrasts in kaolinite and illite clays: Characterization by infrared and X-ray absorption spectroscopies", *Clays and Clay Minerals,* 45(2), 184-193 (1997)

62. J. L. Bantignies, C.C.D.Moulin, H.Dexpert "Asphaltene adsorption on kaolinite characterized by infrared and X-ray absorption spectroscopies", *Journal of Petroleum Science & Engineering,* 20(3), 233-237 (1998)

63. A. Saada, B. Siffert, E.Papirer "Comparison of the hydrophilicity/ hydrophobicity of illites and kaolinites", *Journal of Colloid and Interface Science,* 174(1), 185-190 (1995)

64. V. Bolis, B. Fubini, L. Marchese, G. Martra, D. Costa , "Hydrophilic and

hydrophobic sites on dehydroated crystalline and amorphous silicas", *Journal of the Chemical Society. Faraday Transactions,* 87(3), 497-505 (1991)

65. S. Kondo, K. Tomoi, C. Pak, "Characterization of the hydroxyl surface of silica-gel ", *Bulletin of the Chemical Society of Japan,* 52(7), 2046-2050 (1979)

66. L. Zhu, Y, Feng, X. Ye, Z, Zhou, "Tuning wettability and getting super hydrophobic surface by controlling surface roughness with well-designed microstructures", *Sensors and Actuators. A, Physical,* 130-131, 595-600 (2006)

67. H. Nakae, M. Yoshida, M. Yokota, "Effects of roughness pitch of surfaces on their wettability", *Journal of materials science,* 40(9-10), 2287-2293 (2005)

68. R. Shuttleworth and G. Bailey, "The spreading of a liquid over a rough solids", *Discussions of The Faraday Society,* 3, 16-22 (1948)

69. S. Ren, T. Dang-Vu, H. Y. Zhao, "Effect of weathering on surface characteristics of solids and bitumen from oil sands", Energy & Fuels, 23(1), 334-341 (2009)

APPENDIX I
SUMMARY OF LITERATURE ON THE CLAY
MINERALOGY OF THE ATHABASCA OIL SANDS[12]

Refs.	Reported mineralogy of clay (<2 μm) fraction	Sample source and stream investigated
Bayliss and Levinson (1976)	Kaolinite, illite, up to 10% mixed layers, up to 6% chlorite and up to 1% montmorillonite	247 core ore samples
Camp (1976a,b)	Kaolinite, illite, mixed-layer clays, chlorite and smectite	Ore and fine tailings
Yong and Sethi (1978)	Kaolinite, illite, mixed-layer clays, chlorite and smectite, up to 4% amorphous Fe2O3	SUNCOR pond fine tailings
Kessick (1979)	Kaolinite, illite	Extraction tailings
Dusseault and Scafe (1979)	Illite, kaolinite, vermiculite, illite-vermiculite, kaolinite-vermiculite	Outcrop and borehole ore samples in McMurray formation
Roberts et al. (1980)	Kaolinite, illite, 0.9–3% smectite, 1–6% chlorite, 0.1–6% mixed layer clays	Suncor pond fine tailings
Ignasiak et al. (1983	Kaolinite, illite/smectite (<10% smectite interlayers)	Froth solids
Kotlyar et al. (1984)	Kaolinite, illite	Ore and froth solids
Kotlyar et al. (1985)	Kaolinite, illite	Froth solids
Ignasiak et al. (1985)	Kaolinite, illite, trace amounts of chlorite and smectite in some samples	Ore

Scott et al. (1985)	Kaolinite and illite trace quantities of smectite vermiculite, chlorite and mixed layer clays	Ore and fine tailings
Kotlyar et al. (1987)	Kaolinite, illite, up to 90% amorphous minerals	Ore
Dusseault et al. (1989)	Kaolinite, illite, smectites, vermiculites, mixed layered clays	ore samples from various formations
Kotlyar et al. (1990)	Kaolinite, illite, up to 92% poorly crystalline minerals	Syncrude estuarine and marine ore
Ripmeester et al. (1993	Kaolinite, illite, trace amounts of smectites	fine tailings
Kotlyar et al. (1993)	Kaolinite, illite, trace amounts of smectite and vermiculite	Suncor fine tailings
Cloutis et al. (1995)	Kaolinite, illite	Oil sand samples from Syncrude and Suncor leases
Kotlyar et al. (1995)	Kaolinite, illite	Suncor fine tailings
Dudas (1998)	Kaolinite, hydrous mica	5 fine tailings samples from Suncor, Syncrude and Oslo
Omotoso et al. (2002)	Kaolinite, illite, mixed layer clays (kaolinite-smectite/illite-smectite)	Mature fine tailings from Syncrude and Suncor ponds
Omotoso et al. (2004)	Kaolinite, illite, mixed layer clays chlorite (in some samples)	Mature fine tailings from Syncrude pond, thickener overflow and froth tailings
Wallace et al. (2004)	Kaolinite, "degraded illite"	Ore samples

Omotoso et al. (2006)	Kaolinite, illite, mixed layer clays (kaolinite-smectite/illite-smectite), trace amounts of discrete smectite in marine ores	61 ore samples, 22 froth samples, 54 tailings samples from 3 different leases
Mercier et al. (2008)	Kaolinite, illite	Syncrude fine tailings

APPENDIX II
PROCEDURE OF BITUMEN FLOTATION TESTS

1. Wear personal protective equipment; safety glasses, gloves and lab coat.

2. De-frost a bag of oil sand sample, note the I.D. on the work sheet.

3. With the agitator raised, turn on the agitation and adjust to 1500 rpm, then turn it off. Open the air line (bench valve) and the air stopcock on agitator. Adjust the flow meter to the desired rate (black ball at 80 = 150 ml/min). Then turn off the air stopcock on the agitator only.

4. Using the 1 litre flotation cell, add 300 g of oil sand then 950 ml of tap water.

5. Place the prepared sample in the agitator. While holding the crank handle apply some pressure to release the locking mechanism on the other side. Carefully lower the agitator into the sample till the agitator comes to rest.

6. Put the first bread pan under the lip of the flotation cell.

7. Start agitation for 5 minutes (oil sand conditioning stage). Use the stopwatch. During this time, record the initial temperature. Do not collect any froth.

8. Turn on the air (stopcock on agitator); double check that the flow rate is correct.

9. Use a spatula to start collecting the bitumen froth floating on the slurry surface into a container (bread pan) for 3 minutes. Try not to drag too much water into the pan. Continue collecting the froth into a second pan for 2 minutes (5 minutes total). Finally, collect into a third pan for another 5 minutes (10 minutes total from initial aeration).

10. Turn off the aeration and agitation. Place the three collected froth containers aside.

11. Holding the locking mechanism out, raise the flotation cell to its maximum height and re-lock in place. Transfer the flotation tailings to a one litre graduated cylinder and set aside for settling (for zeta potential analysis). After 30 minutes, use a pipette to draw 10 ml of the tailings water for zeta potential analysis. Also, fill four 50 ml centrifuge tubes with the tailings water and centrifuge at 10,000 g for

10 minutes. Set this clarified (process water) aside to use for zeta potential analysis of the froth and tailings.

12. Re-mount the cell under the agitator. Lower the shaft part way into the cell and wash with tap water. Raise it again and pour the wash water and remaining tailings into the waste pail. Re-mount the cell and lower the agitator to the bottom.

13. Put toluene into the cell, turn on the agitation for a few minutes to remove and wash away any bitumen stuck on the shaft, inside the rotator and on the cell. Raise the agitator and pour waste toluene into an organics only waste container.

APPENDIX III
PROCEDURE OF DEAN STARK ANALYSIS

1. Wear personal protective equipment; safety glasses, gloves and lab coat.

2. Add about 200 ml of toluene to each of the three flasks to be used.

3. Label and place a thimble into a labeled jar for each of the three froth samples to be tested. Weigh thimble plus jar for each sample.

4. Weigh 2 Kimwipes for each of the three samples. Use Kimwipes to wipe any bitumen left in the bread pans.

5. Carefully transfer the collected froth from the bread pans to each thimble with the spoon.

6. Using the Kimwipes, wipe the remaining sample from the pan and add the Kimwipes to the thimble.

7. Weigh individually the three jars containing the froth sample.

8. Transfer the thimbles to the flasks using the baskets and hang on the adapter. Cover the top of the thimble with the small screen before inserting them into the flask.

9. Attach the trap and condenser. Be sure the trap stopcock is closed.

10. Turn on the condenser water. Ensure a good flow rate of water through condensers and check for leaks.

11. Turn on the heating mantles to level 9 to begin boiling and refluxing.

12. Label and weigh each of the three plastic water bottles. Each bottle is for a given Dean Stark flask.

13. As water is collected in the trap, the level may rise to the top of the trap. Drain some of the water into the water bottle to again see an interface between the toluene and the water.

14. Continue refluxing for one hour or until the toluene dripping from the thimble is colorless. Periodically check the bottom of the flask so it doesn't get too low. Add toluene if necessary.

15. Turn off the mantles and leave condenser water on until the apparatus is cool for at least 1 hour.

16. Collect the water from the traps and weigh the plastic bottles.

17. Empty the traps into the toluene waste container.

18. Transfer the thimbles back into the glass jars and place in the vacuum oven to dry over night.

19. Transfer the liquid from the Dean Stark to 250 ml flasks, rinse with toluene wash bottle and ensure not to overfill the flask past the volumetric mark.

20. Allow the flask to cool and add toluene to the 250 ml mark.

21. Shake the flasks holding the stopper.

22. Weigh filter paper.

23. Pipette 5 ml from the 250ml flask onto filter paper placed on a watch glass. Use a side to side motion to evenly saturate the filter paper leaving a top portion dry in order to hang it.

24. Start the stop watch and hang the saturated filter paper in the fume hood by the paper clip.

25. After 20 minutes weigh the filter paper.

26. Empty the 250ml flasks into organic waste container.

27. The next day, weigh the dried thimbles and their content.

APPENDIX IV
BULK & CLAY XRD ANALYSIS PROCEDURES

1. Crush dry sample until grains disintegrate completely.

2. Weigh empty beaker and put sample in it. Weigh again "total weight".($\approx$ 3g of sample).

3. Add 50 mL of distilled water, plus a few drops of Sodium Metaphosphate.

4. Put in ultrasonic bath for 2 hours.

5. Stir sample and pour out top portion into test tube.

6. Centrifuge for 5 minutes at 600 rpm.

7. Pour out top portion into another test tube for the clay fraction (<3μm) sample

8. Recombine the coarser residue in the first test tube with the residue in the beaker and weight this "bulk sample" (after drying completely). Subtract this weight from the "total weight" to get the clay fraction weight.

9. Centrifuge the "clay fines" in the second test tube for 20 minutes at maximum rpms.

10. Pour out most of the water then shake test tube using Vortex Mixer.

11. Pipette onto a glass slide.

12. Put the slide on the hot plate (low) until dry then run sample in XRD.

13. Then put slide in a glycol vapour bath overnight (glycolated clay); Smectite will swell and be recognized.

14. If chlorite suspected, then treat the remaining sample in the test tube with diluted HCl and leave overnight (acidized clay). If chlorite was present in the sample this test causes it to disappear.

15. Run the "clay fraction" slide from 2-38 degrees. Grind the "bulk sample" and spread the powder on an aluminum holder then run from 4-58 degrees.

APPENDIX V
XRD ANALYSIS RESULTS

SAMPLE ID	TYPE OF ANALYSIS	WEIGHT %	Qtz	Plag	K-Fled	Cal	Dol	Anhy	Pry	Hal	Bar	Sider	Kaol	Chl	Ill	ML	Smec
	BULK FRACTION	63.04	5	0	3	0	0	0	25	0	0	31	22	0	14	0	0
OWS-T	CLAY FRACTION	36.96	0	0	0	0	0	0	0	0	0	0	74	0	26	0	0
	BULK AND CLAY	100	3	0	2	0	0	0	16	0	0	20	41	0	18	0	0
	BULK FRACTION	73.33	7	0	3	0	0	0	24	0	0	35	31	0	0	0	0
OWS-H	CLAY FRACTION	26.67	0	0	0	0	0	0	0	0	0	0	80	0	20	0	0
	BULK AND CLAY	100	5	0	2	0	0	0	18	0	0	26	44	0	5	0	0
	BULK FRACTION	60.87	12	0	0	0	0	0	1	0	0	6	60	0	21	0	0
WWS-T	CLAY FRACTION	39.13	0	0	0	0	0	0	0	0	0	0	71	0	29	0	0
	BULK AND CLAY	100	8	0	0	0	0	0	1	0	0	4	63	0	24	0	0
	BULK FRACTION	73.91	10	0	0	0	0	0	1	0	0	5	64	0	20	0	0
WWS-H	CLAY FRACTION	26.09	0	0	0	0	0	0	0	0	0	0	63	0	37	0	0
	BULK FRACTION	100	7	0	0	0	0	0	1	0	0	4	64	0	24	0	0

Abréviations

Anhy - Anhydrite   Cal - Calcite   Chl - Chlorite   Dol - Dolomite

Ill - Illite   Kaol - Kaolinite   K-feld - Potassic Feldspar

ML-Mixed-layer clays Plag - Plagioclase   Pyr -Pyrite   Qtz – Quartz

Sider - Siderite   Smec-Smectite